Statistics of Extreme Events with Application to Climate

H. Abarbanel
S. Koonin
H. Levine
G. MacDonald
O. Rothaus

January 1992

JSR-90-305

JASON
The MITRE Corporation
7525 Colshire Drive
McLean, Virginia 22102-3481
(703) 883-6997

REPORT DOCUMENTATION PAGE

Form Approved
OMB No. 0704-0188

1. AGENCY USE ONLY (Leave blank)	2. REPORT DATE	3. REPORT TYPE AND DATES COVERED
	January 10, 1992	

4. TITLE AND SUBTITLE

Statistics of Extreme Events with Application to Climate

5. FUNDING NUMBERS

PR - 8503Z

6. AUTHOR(S)

G. MacDonald, et al

7. PERFORMING ORGANIZATION NAME(S) AND ADDRESS(ES)

The MITRE Corporation
JASON Program Office A10
7525 Colshire Drive
McLean, VA 22102

8. PERFORMING ORGANIZATION REPORT NUMBER

JSR-90-305

9. SPONSORING/MONITORING AGENCY NAME(S) AND ADDRESS(ES)

Department of Energy
Washington, DC 20585

10. SPONSORING/MONITORING AGENCY REPORT NUMBER

JSR-90-305

11. SUPPLEMENTARY NOTES

12a. DISTRIBUTION/AVAILABILITY STATEMENT

Distribution unlimited; open for public release.

12b. DISTRIBUTION CODE

13. ABSTRACT *(Maximum 200 words)*

The statistical theory of extreme events is applied to observed global average temperature records and to simplified models of climate. Both hands of records exhibit behavior in the tails of the distribution that would be expected from a random variable having a normal distribution. A simple nonlinear model of climate due to Lorenz is used to demonstrate that the physical dimensions of the underlying attractor, determined by applicable conservation laws, limits the range of extremes. These limits are not reached in either observed series or in more complex models of climate. The effect of a shift in mean on the frequency of extremes is discussed with special reference to possible thresholds for damage to climate variability.

14. SUBJECT TERMS

bernoulli trials, non-parametric order statistics, asymptotic distribution, Lorenz 27-variable

15. NUMBER OF PAGES

16. PRICE CODE

17. SECURITY CLASSIFICATION OF REPORT	18. SECURITY CLASSIFICATION OF THIS PAGE	19. SECURITY CLASSIFICATION OF ABSTRACT	20. LIMITATION OF ABSTRACT
UNCLASSIFIED	UNCLASSIFIED	UNCLASSIFIED	SAR

Contents

1 INTRODUCTION

The social and economic costs associated with global warming will be measured in terms of changes in the frequency and intensity of extreme events such as droughts, floods, hurricanes, tidal surges, etc. Small changes in the mean temperature are easily adjusted to, but successive years of drought or a sequence of storms are much less easily handled even by advanced societies. The capability to forecast the frequency and intensity of extreme events in an altered atmosphere poses a great challenge.

In the statistical literature the large or small values assumed by a random variable from a finite set of measurements are termed extreme values. The variable of interest could be sea level, atmospheric temperature, precipitation, stream flow, etc. The largest and smallest value of the extremes are often of most interest. However, other extremes such as the second or third largest or smallest may be of interest. The extreme values are random variables. For example, the minimum temperature in January in Bismarck, North Dakota, exhibits random variations that are best described in terms of probabilities.

The application of extreme value statistics is uncommon in the environmental sciences except in the field of hydrology, where the concepts have been used in designing dams. As noted in Levine et al. (1990), extreme value theory has not received much attention in climate studies or in discussions of greenhouse warming despite the obvious importance of large deviations from

the mean. The theory and applications are rarely treated in books on probability and statistics and almost never covered in university courses. If there are references to the subject, it is generally to Gumbel's (1958) book which has long been out of print. Cramér and Leadbetter (1967) and Leadbetter, Lindgren and Rootzen (1982) provide an extensive treatment of extremes in stationary sequences but focus primarily on certain of the difficult mathematical issues related to extreme values. The statistics of extremes is closely connected to order statistics which provides an approach to distribution free or robust statistics (David, 1981). The present paper provides a review of the theory with a number of applications that are related to climate change issues.

The applications are both to real data – time series of temperature derived from various sources – and to results obtained from much simplified computer models of climate. The latter application is primarily to provide an illustration of how the problem of extremes can be approached, rather than to give definite answers. Some of the examples could be extended to data derived from large scale global circulation models (GCMs) of the atmosphere, but since we do not have access to GCMs we have not done so.

Sections 2, 3 and 4 serve to introduce the nomenclature of order statistics with a few elementary examples of the calculation of the probability of extreme climatic events. In Section 5, results from order statistics are applied to calculate the probability that the observed global average surface air temperature records contain a trend. Unlike a previous analysis (Levine et al., 1990), no assumption is made as to the underlying statistical distribution.

Since extremes are rare events they can be approximated as independent with negligible correlation. In accord with the earlier analysis (Levine et al., 1990), order statistics indicate very high odds ($10^5 - 10^6$ to 1) in favor of the hypothesis that the data records contain a linearly increasing trend in global average surface air temperature.

Section 6 presents an introductory discussion of the distribution of extremes with no restricting assumptions as to the distribution of the parent population. While general results can be obtained, detailed applications require assumptions as to the underlying distribution. The theory is specialized in Section 7 to normal distributions. An application to the Lorenz 27-variable model of climate shows that the temperature values calculated for the Lorenz model closely approximate normally distributed variates both about the mean and in the tails (extremes) of the distribution for a run of 1000 years.

For a normally distributed random variable, the range (maximum minus minimum) increases without limit as the number, n, of variates selected increases (as $(ln\ n)^{1/2}$). Section 7.2 provides an example where the physical dimension of the underlying attractor limits the growth in range with time. This limit is not observed in model runs or in observed temperature records (see Sections 7.3 and 7.4). Both model runs and observed temperature records from which a trend has been removed closely approximate normally distributed variates about the mean and in the tails of the distribution. These results raise questions as to the predictability of climate.

The effect of a shift in mean on the frequency of extremes is discussed

in Section 8 with special reference to possible thresholds for damage due to climate variability. Section 9 provides a brief summary of the major findings of the report.

2 RETURN PERIOD

Engineers who design dams are interested in the time interval between two discharges of a river, each of which is greater than or equal to a given discharge. The probability p of a random variate X having a value greater than x is

$$\begin{aligned} p = 1 - F(x) &= 1 - \int_{-\infty}^{x} f(y)\, dy \\ F(x) &= Pr(X \leq x) \end{aligned}$$

where $F(x)$ is the cumulative probability function and $f(x)$ is the probability density function. We are interested in the number of independent trials k before the value x is exceeded. The variable k is an integer limited on the left but not on the right, since the value of x may never be surpassed. The probability that x is first exceeded at trial k is

$$p(1-p)^{k-1} = p\, q^{k-1}$$

since the event failed for the first k–1 trials (Bernoulli trials). The mean for k is simply

$$E\,[k] = 1/p = \frac{1}{1 - F(x)} > 1.$$

The return period is defined by

$$T(x) \equiv \frac{1}{1 - F(x)}.$$

If an event has probability p, on the average we have to make $1/p$ trials in order for the event to happen once.

The standard deviation for k is

$$\sigma = \sqrt{2}\,(T^2 - T)^{1/2}$$

which for a long return period becomes

$$\sigma \simeq \sqrt{2}\,(T - \frac{1}{2}).$$

The smaller the probability of an event, the larger the spread of the distribution. This general property lessens the usefulness of extremes in numerous situations.

The cumulative probability W(k) that the event happens before or at the kth trial is

$$W(k) = 1 - (1 - p)^k.$$

The probability that the event will happen before its return period T is

$$\begin{aligned} W(T) &= 1 - (1 - \frac{1}{T})^T \\ &\approx 1 - \frac{1}{e} = 0.6231. \end{aligned}$$

If the value to be exceeded, x, is large and the return period long, say greater than 10, then the cumulative probability W(k) can be approximated by

$$W(k) \simeq 1 - \exp(-\frac{k}{T}).$$

In hydrology the return period is usually measured in years. For example, a design engineer may wish to have a high probability (0.95) that an event does not happen in N years. The return period T for the design is then

approximately

$$T = \frac{N}{1 - W}$$

so that in order to have a probability of 1 in 20 that the event does not happen in 10 years requires the design to have a much larger return period of 200 years.

These simple considerations illustrate certain features of the statistics of extremes. Under the assumption that the events are independent, results can be obtained that are free of any assumption with respect to the underlying distribution. The assumption of independence might appear to be highly restrictive. For dependent variables, their correlation as a function of time difference or lag is a partial measure of their dependence. Many of the results derived for independent variables apply to dependent variables provided that the correlation decreases rapidly enough with lag (Leadbetter, Lindgren and Rootzen, 1983). The basic reason for applicability of results obtained from the theory of independent events to correlated series is that extreme events are rare. Rare events are expected to be separated by long time intervals so that the effects of correlation are negligible. If the correlation function decays at least as fast as $1/ln\ n$ where n is the time, then the effects of the correlation can be neglected as is discussed by Leadbetter, Lindgren and Rootzen (1983).

3 FREQUENCY OF EXCEEDANCES

3.1 Bernoulli Trials

The statistics of Bernoulli trials can easily be applied to extreme events. The probability that during the next n years the maximum July temperature in Washington, D.C., will exceed 105°F exactly k times is

$$P_k = \binom{n}{k} p^{n-k} (1-p)^k$$

where p, estimated on past observations, is the probability that the maximum July temperature will not exceed 105°F and where

$$\binom{n}{k} = \frac{n!}{(n-k)!\, k!}$$

is the binomial coefficient. The probability of exceeding 105°F in Washington is about a 1 in 20- year event, $p = 0.95$. In the next decade, provided that there is no upward or downward trend in temperatures, the probability that the maximum July temperature will not exceed 105°F is

$$P_0 = \binom{10}{0} (0.95)^{10} (0.05)^0 = 0.6$$

or there is a 40 percent chance that the maximum July temperature will exceed 105°F in the period 1990-1999.

The probability that during the next ten years there will be fewer than three years for which the maximum temperature for July exceeds 105°F can

also be calculated. There are only three ways that the number of exceedances of 105°F cannot be greater than two — namely when the number is zero, one or two. The probability of these mutually exclusive events is the sum of the probabilities of each

$$P_0 + P_1 + P_2 = \binom{10}{0} (0.95)^{10} (0.05)^0 + \binom{10}{1} (0.95)^9 (0.05) + \binom{10}{2} (0.95)^8 (0.05)^2 = 0.9885.$$

The probability of the maximum July temperature in Washington in the next decade exceeding 105°F three or more times is only 1 in a 100. If in the next decade the temperature does exceed 105°F in July three or more times, the hypothesis that there is no upward trend in the temperature should be reexamined.

The number of exceedances depends on the interval over which the observations are made. From the results of the above example we can calculate the probability that over the next century every decade will have no more than two Julys in which the maximum temperature exceeds 105°F. With a shift in time scale the probability is

$$P = \binom{10}{0} (0.9885)^{10} (1 - 0.9885)^0 = 0.89.$$

4 NON-PARAMETRIC ORDER STATISTICS

The need to estimate the probability p_m of the mth ranked observation can be avoided by using past observations to determine the exceedances in future trials. Let n denote the number of past observations, N the number of future observations, m the rank of the ordered past observation and k the number of exceedances of the mth ranked observation in N future trials. The probability of observing in N trials, k exceedances of the mth ranked observation seen in n trials is:

$$\begin{aligned} P(k;n,m,N) &= \binom{N}{k}\binom{n}{m} m \int_0^1 p^{N-k}\,(1-p)^k\,p^{n-m}\,(1-p)^{m-1}dp \\ &= \frac{\binom{n}{m}\binom{N}{k} m}{(N+n)\,\binom{N+n-1}{m+k-1}} \end{aligned}$$

since the integral is a special case of the Beta integral

$$\beta(j,k) = \int_0^1 (1-y)^{j-1}\,y^{k-1}dy = \frac{\Gamma(j)\Gamma(k)}{\Gamma(j+k)}.$$

For the largest value, $m = 1$, the probability of k exceedances is

$$P(k;n,1,N) = \frac{nN!(N+n-k-1)!}{(N-k)!\,(N+n)\,(N+n-1)!}.$$

The probability that the maximum value observed in n trials is not exceeded in N future trials is

$$P(0;n,1,N) = \frac{n}{N+n},$$

and there is 0.5 probability that the maximum is not exceeded in an equal number, $N = n$, of future trials. The calculation of the probabilities for the exceedance of the largest value is aided by the recursion relation

$$P(k+1;n,1,N) = \frac{(N+1-k)}{(N+n-k)}\, P(k;n,1,N).$$

The probability that all values in N future trials will exceed the largest value observed in the first n trials is small. For the case $N = n$, this probability is

$$P(N;N,1,n) = \frac{(N!)^2}{(2N)!}$$

which for $N = 6$ is 0.00108.

The various moments of the distribution function can be obtained from properties of the hypergeometric function (Gumbel, 1954). The mean number of exceedances is

$$\begin{aligned} E\,(n,m,N) &= \sum_{k=1}^{N} k\, P(k;n,m,N) \\ &= mN/(n+1). \end{aligned}$$

Similarly, the variance of the estimate of the number of exceedances is

$$\sigma^2\,(n,m,N) = \frac{m(n-m+1)\; N(N+n+1)}{(n+1)^2(n+2)}.$$

The variance increases with the number, N, of future trials and decreases with the number of past observations used to set up the statistics. The variance for the number of exceedances of the maximum is

$$\sigma^2(n,1,N) = \frac{nN(N+n+1)}{(n+1)^2\,(n+2)}.$$

The variance of the estimate for the median, $m = \frac{n+1}{2}$, n odd, is

$$\sigma^2(n, \frac{n+1}{2}, N) = \frac{N(N+n+1)}{4(n+2)}$$

so that the ratio of the variance of the estimated number of exceedances of the maximum to the number of exceedances of the median is

$$\frac{\sigma^2(n,1,N)}{\sigma^2(N,\frac{n+1}{2},N)} = \frac{4n}{(n+1)^2}.$$

In one sense, the extremes are more reliable than the median since the variance of the number of exceedances of the median is about $\frac{1}{4}n$ as large as the variance for the maximum. In the limit of large N with $N = m$ the mean and the variance take on simple forms

$$E[k] \simeq m$$

and

$$\sigma^2(n, m, N) \simeq 2m.$$

The mean number of exceedances over the mth largest value is equal to the rank m itself. The distribution is then similar to a Poisson distribution for integers. However, the variance is twice that of a Poisson distribution. The probability distribution of exceedances in this case is independent of the distribution of the random variable X. It does depend on the assumption that the observations are independent. The lack of dependence on the distribution is an attractive feature of the theory, since the distribution may be known in the vicinity of the median but there will, in most cases, be very few observations with regard to extreme values.

5 APPLICATIONS OF ORDER STATISTICS TO GLOBAL AVERAGE TEMPERATURE

A 109-year record of the annual global average temperature of the atmosphere has been determined by Hansen and Lebedeff (1987, 1988) (see Figure 1). The data have been normalized to zero mean. The maximum temperature for the 100-year period 1880-1979 is 0.2°C, observed in 1954. The probability of one or more exceedances of the maximum of this 100-year record in the nine-year period 1980-1988 is

$$P\,(\geq 1; 100, 1, 9) = 1 - \frac{100}{109} = 0.083$$

if the average temperature can be taken as an independent trial and there is no trend. The expected number of exceedances is $E(100, 1, 9) = 9/100 = 0.089$ with a variance of $\sigma^2(100, 1, 9) = 0.095$. In fact there were five exceedances: 1988, 1981, 1987, 1983 and 1980. The probability under the independence assumption of five exceedances is

$$P\,(5; 100, 1, 9) = 1.03 \times 10^{-6}.$$

The observed five exceedances strongly contradict the assumption of independence and provide support for the hypothesis that there is an increasing trend in the annual global average surface temperature.

If a linear trend with a least square slopes of 0.55° per century is removed the maximum residual in the first 100 years is 0.28°C in 1926. There are no exceedances for the years 1980-1988 in the residual as would be expected from

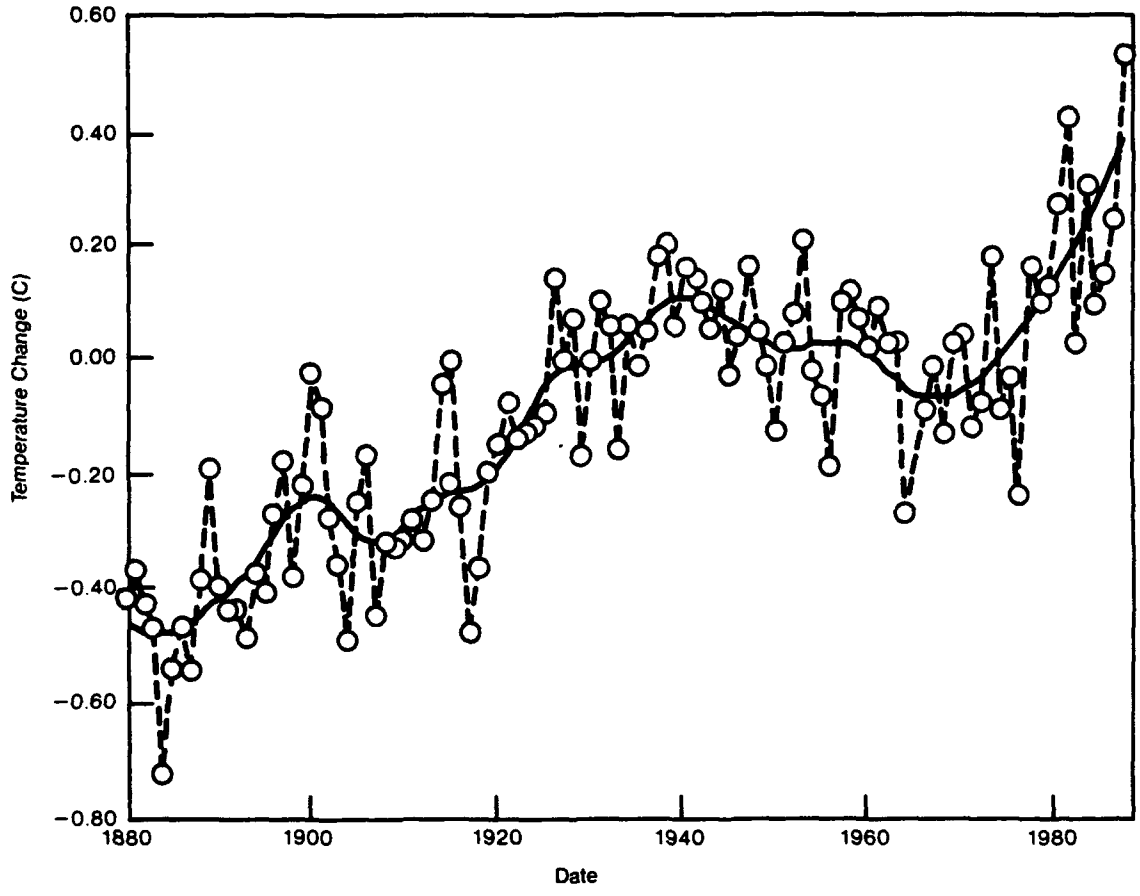

Figure 1. Variations of global average temperature. The solid curve is a filtered version corresponding to a five-year running average (after Hansen and Lebedeff, 1987; 1988).

Table 1

Expected Number of Exceedances in Six-Year Runs of Global Annual Average Temperature and Observed Exceedances in 17 Six-Year Runs

Number of Exceedances k of Maximum Value	Probability of k	Expected Number of Exceedances	Observed Number of Exceedances	Observed Number of Exceedances in Residual after Removal of Linear Trend
0	0.5	8.5	0	2
1	0.273	4.64	1	3
2	0.136	2.31	1	3
3	0.061	1.03	0	4
4	0.027	0.46	2	2
5	0.006	0.11	1	1
6	0.001	0.02	12	2

the probability distribution for the maximum. In terms of odds, the ratio of the probability of the observations containing a trend to the probability that the temperatures are independent, identically distributed random variables is

$$\frac{0.917}{1.03 \times 10^{-6}} = 8.9 \times 10^{5}.$$

As a further example of the use of the probability distribution, the 108-year record, 1980-1987, is divided into 18 consecutive six-year segments. The maximum value in the first six-year period, 1880-1885 is - 0.37°C. The number of exceedances in each of the subsequent six-year segments is tabulated in Table 1 along with the number obtained for the probability distribution.

The expected number of exceedances in any six-year period is

$$E\,(6,1,6) = 6/7 = 0.86$$

with a standard deviation of

$$\sigma = 1.09.$$

Clearly the number of six-year runs with all six values in excess of the maximum for the first six-year segment is much larger, 16, than would be expected from a sequence of independent trials. The probability of obtaining 12 segments out of 17 in which all the values are in excess is

$$\frac{17!}{12!\,5!}\,(0.00108)^{12}\,(1-0.00108)^{5} = 1.5 \times 10^{-32}.$$

Table 1 also tabulates the observed distribution of exceedance for the residuals after a linear trend has been removed. The observed distribution still differs from the calculated one. However, the probability of obtaining two segments in which all six values are greater than the maximum observed in the first six-years while small, 1.5×10^{4}, is much larger than the probability of obtaining 12 such sequences.

Levine et. al (1990) calculated that the odds for a linear trend in the data were 1.7×10^{5} to one. In that analysis, the correlation between annual temperature was explicitly taken into account through the use of the full covariance matrix in the least squares analysis but the analysis was based on the assumption that the global average temperatures were normally distributed. The analysis presented above supports the hypothesis of a trend by similar odds, but is based on the assumption of independent trials without any assumption on the underlying statistical distribution.

6 DISTRIBUTION OF EXTREMES

The above analysis provides information with respect to the number of observations that would exceed the mth largest value of n initial observations. The analysis provides no information on the value that would exceed the observed extremes. Such information requires that the underlying probability distribution, $F(x)$, be known. As illustrated above, some of the analysis of the frequency of exceedances can be carried out without assumptions with respect to the underlying distribution of the random variable. The exact form of the distribution is generally not known, but an asymptotic theory that covers a wide variety of initial distribution has been developed (Cramér, 1946, Gumbel, 1958).

As before, let k denote the kth value from the top of a sample of n observations. The probability density $g(x; n, k)$ for the kth value is equal to the probability that among n samples $n - k$ are less than x, and $k - 1$ are greater than x while the remaining value falls between x and $x + dx$

$$g(x; n, k) = n\binom{n-1}{k-1}[F(x)^{n-k}\,(1 - F(x))^{k-1}]f(x)dx$$

where $F(x)$ is the probability distribution function and $f(x)$ is the density distribution function. For the maximum value $k = 1$ and

$$g(x; n, 1) = [F(x)]^n\, dx.$$

For a population having a normal distribution with zero mean and unit variance

$$F(x) = \frac{1}{\sqrt{2\pi}} \int_{-\infty}^{x} e^{-t^2/2}\, dt.$$

The dependence of the maximum value on the number of observations from a series of independent trials drawn from a normal population is illustrated in Figure 2. For a sample of ten, the maximum has a 0.05 probability of exceeding 2.57 standard deviations; for a sample of 1000, the maximum will exceed 3.89 standard deviations one in twenty times.

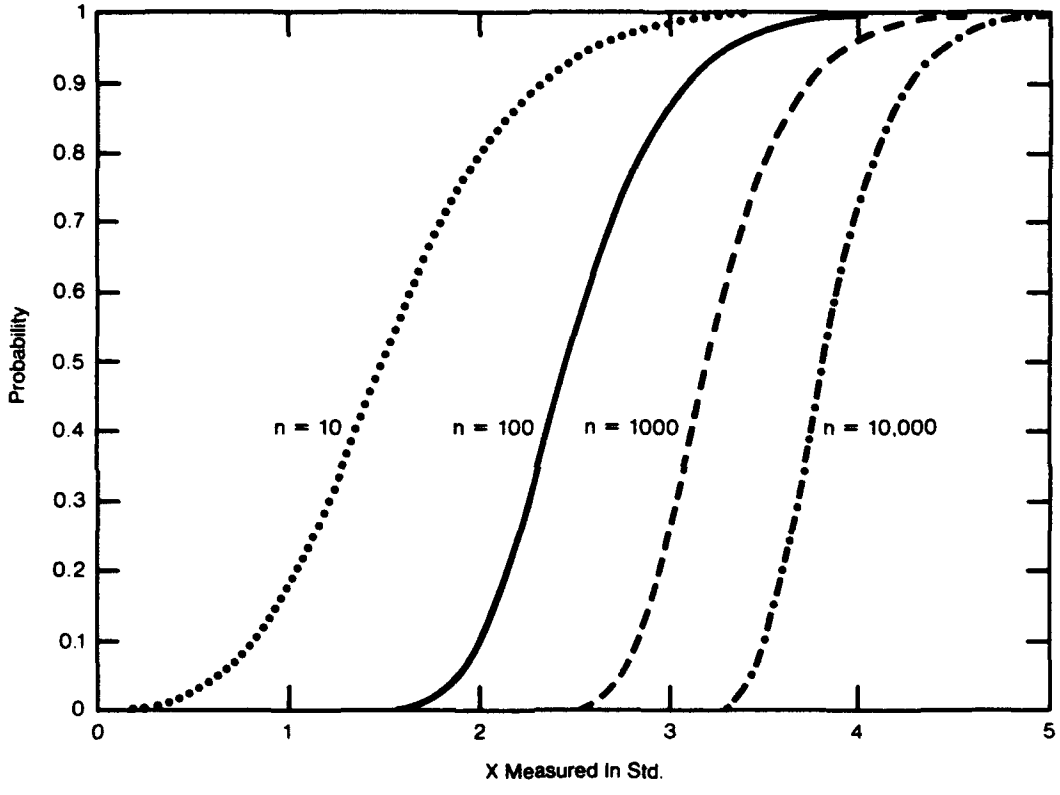

Figure 2. Variations of the probability of the maximum of n independent trials with n. The distribution has zero mean and unit variance.

7 ASYMPTOTIC DISTRIBUTION OF EXTREMES FOR A NORMAL PROCESS

The general asymptotic theory of the distribution of extremes deals with the conditions under which

$$P[a_n(M_n - b_n) \leq x]$$

approaches a limiting distribution G(x) where a_n and b_n are suitable normalizing constants and

$$M_n = \max[X_1, X_2, ..., X_n].$$

The theory states that every distribution G, has, up to scale and location changes, one of the following parametric forms commonly called the Three Extreme Value distributions:

Type I:	$\infty < x < \infty$	$G(x) = \exp(-e^{-x})$
Type II:	$x > 0$	$G(x) = \exp(-x^{-\alpha});\ \alpha > 0$
	$x \leq 0$	$G(x) = 0$
Type III:	$x \leq 0$	$G(x) = \exp(-(-x)^{\alpha});\ \alpha > 0$
	$x > 0$	$= 1$

(Leadbetter, Lindgren and Rootzen, 1983). The normal distribution, unlimited on the left and right, falls into the Type I domain of attraction. The density distribution for the kth ordered value becomes

$$\exp(-x^k - e^{-x})$$

which is illustrated in Figure 3 for $k = 1, 2, 3$.

For a normal distribution with zero mean and unit variance, if x is the

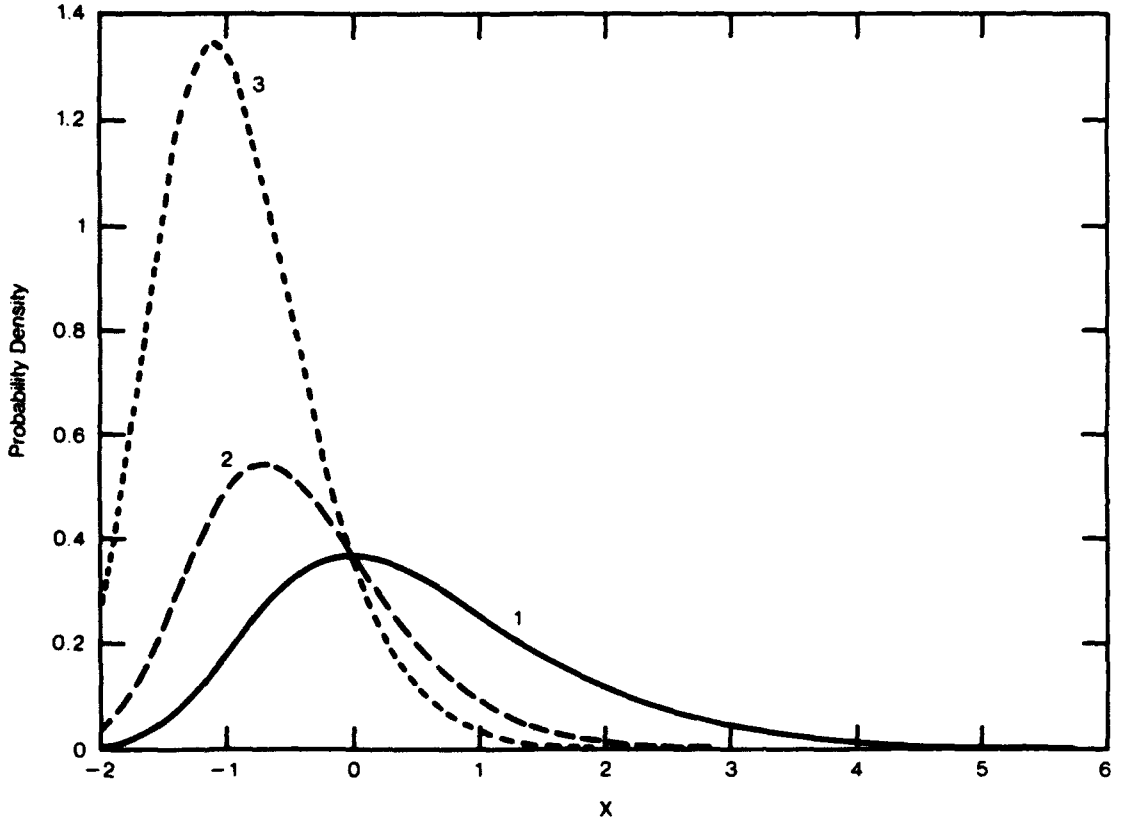

Figure 3. The probability density function for the double exponential.

kth value from the top, then ξ is

$$\xi = \frac{n}{\sqrt{2\pi}} \int_x^\infty e^{-t^2/2} dt.$$

The normalizing constants can be obtained by a complex calculation. The solution for x when n is large can be obtained by partial integration leading to

$$\frac{\sqrt{2\pi}\xi}{n} = \frac{1}{x} e^{-\frac{x^2}{2}} + 0(\frac{1}{x^2}) e^{-x^2/2}.$$

With bounded ξ, x is given by

$$x = (2 \ln n)^{1/2} - \frac{\ln \ln n + \ln 4\pi}{2(2 \ln n)^{1/2}} - \frac{\ln \xi}{(2 \ln n)^{1/2}} + 0(\frac{1}{\ln n}).$$

For the general form of the normal distribution with arbitrary mean m and variance σ^2, the form for $M_n = x$ is asymptotically

$$x = m + \sigma(2 \ln n)^{1/2} - \sigma\frac{\ln \ln n + \ln 4\pi}{2(2 \ln n)^{1/2}} + \frac{\sigma v}{(2 \ln n)^{1/2}}$$

where v is a random variable having the frequency function

$$\exp(-x^k - e^{-x}).$$

The expression for the kth value from the bottom is given by a similar expression with opposite sign for all terms but the mean, m.

The expected value for the kth value from the top is

$$E[x; n, k] = m + \sigma\left(2 \ln n)^{1/2} - \frac{\ln \ln n + \ln 4\pi + 2(S_1 - C)}{(2 \ln n)^{1/2}} + 0(\frac{1}{\ln n})\right)$$

with variance D^2

$$D^2(x; n, k) = \frac{\sigma^2}{2 \ln n}\left(\frac{\pi^2}{6} - S_2\right) + 0\left(\frac{1}{\ln^2 n}\right)$$

where C is Euler's constant, C=0.57722...,

$$S_1 = \frac{1}{1} + \frac{1}{2} + \cdots + \frac{1}{k-1}$$
$$S_2 = \frac{1}{1^2} + \frac{1}{2^2} + \cdots + \frac{1}{(k-1)^2}.$$

Similar expressions can be calculated for the difference between the kth maximum and kth minimum values of the n independent trials drawn from a normal population.

$$E[x-y;n,k] = \sigma\left(\frac{4\ ln\ n - ln\ ln\ n - ln\ 4\pi - 2(S_1 - C)}{(2\ ln\ n)^{1/2}} + 0(\frac{1}{ln\ n})\right)$$
$$D^2[x-y;n,k] = \frac{\sigma^2}{ln\ n}(\frac{\pi^2}{6} - S_2) + 0(\frac{1}{ln^2\ n}).$$

The dependence of the range on the number of observations is indicated in Figure 4. The three standard deviation bounds are also shown. For a normal population of a 1000 variables there is about 1 in a 100 probability that the maximum range will exceed eight standard deviations. The expected value for the maximum of normal population is shown in Figure 5.

7.1 Applications of Asymptotic Theory of Extremes to a Climate Model

The variation of global average annual temperature depicted in Figure 1 shows irregular behavior with a non-vanishing correlation function for lags up to the length of the record and continuous power spectrum with abundant energy at low frequencies (Levine et.al, 1990). The irregular behavior, characteristic of chaotic systems, also shows clearly in complex models of the

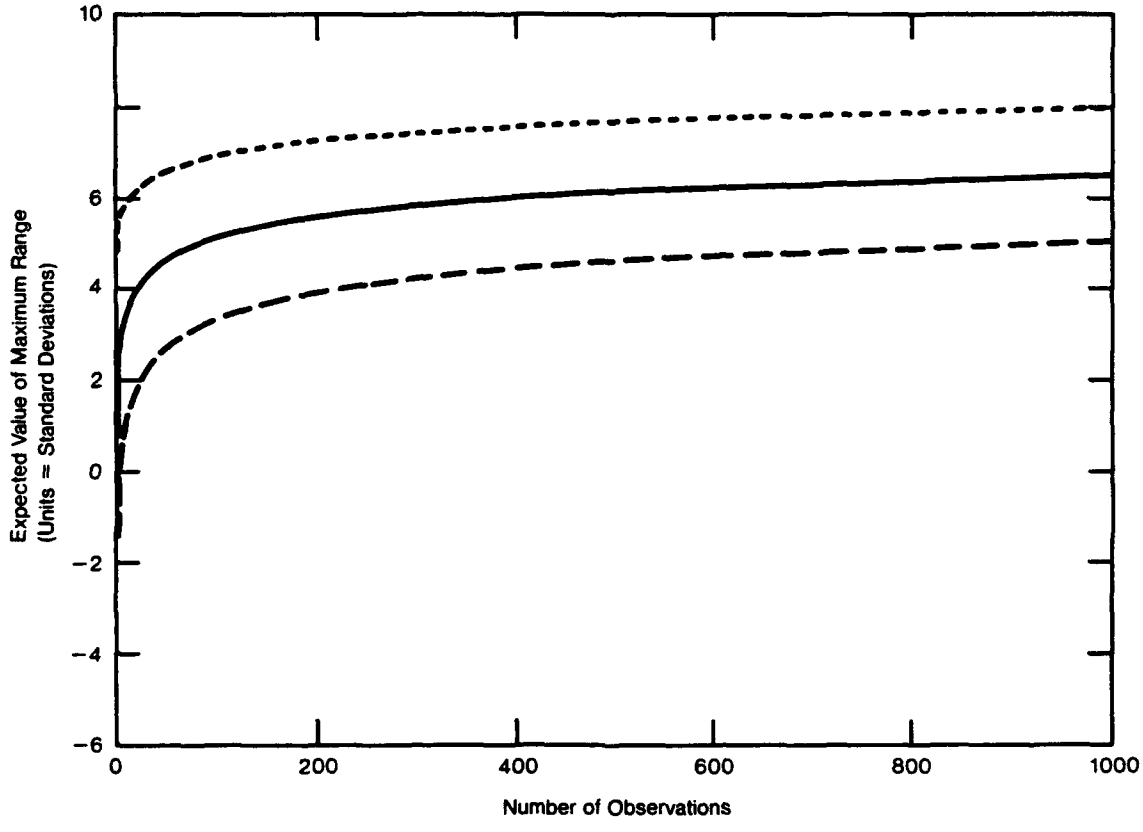

Figure 4. Variations of the maximum expected range for a random variate drawn from a normal population as a function of the number of observations. The distribution has zero mean and unit variance. The three standard deviations from the expected value are also shown.

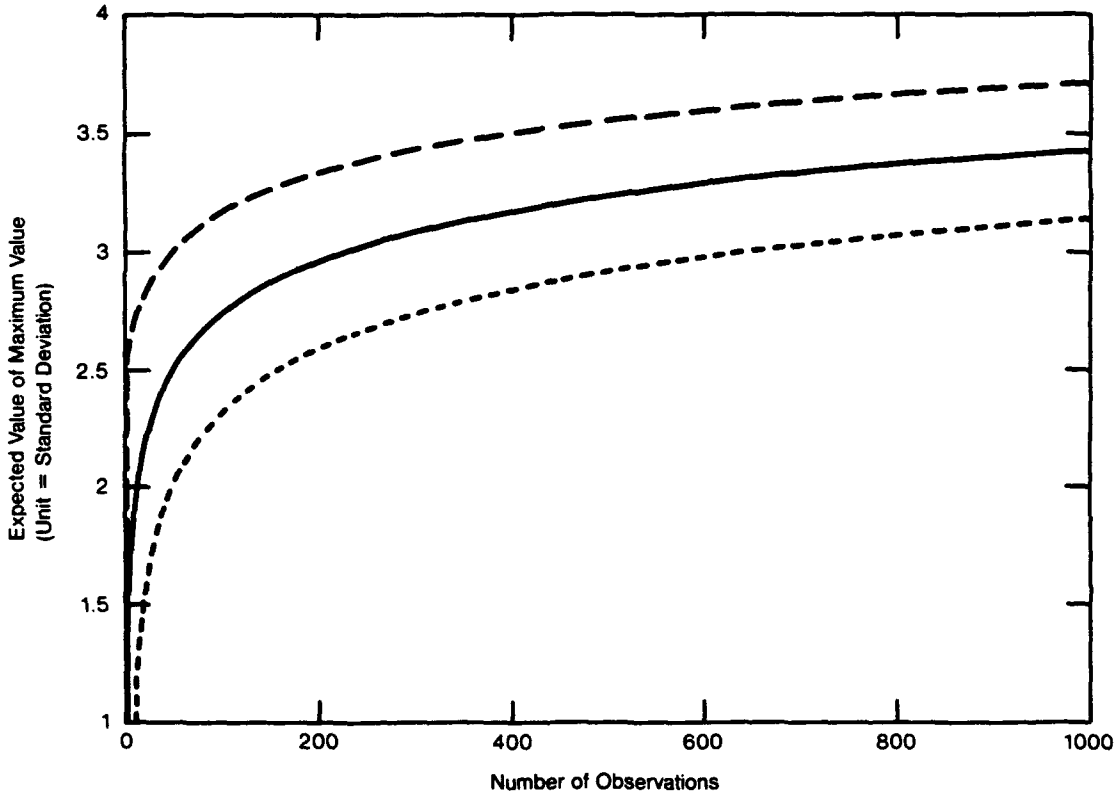

Figure 5. Variation in expected maximum value of an observation drawn from a normal population with zero mean and unit variance as a function of the number of observations. The three standard deviations from the expected value are also shown.

atmosphere such as General Circulation Models, which contain about 100,000 coupled nonlinear equations, and also in the simplest models. Lorenz (1984a) has developed a low-order model in 27 variables that has been analyzed in some detail by Levine et al.,(1990). The physical variables include the mixing ratios of water vapor and liquid water as well as temperature, pressure and the usual dynamic variables. In the Lorenz model, the atmosphere and ocean exchange heat and water through evaporation and precipitation. The model also produces clouds, which reflect incoming solar radiation, while both phases of water absorb and re-emit infrared radiation.

For a 1000-year run for the global average annual temperature, the observed standard deviation was 0.3583°C. The data scaled to unit variance and zero mean are shown in Figure 6. The observed maximum value is 3.407. The probability of obtaining this value with 1000 values is 0.712, or a probability of 0.29 that 3.4 would be exceeded in a 1000-year run of independent trials drawn from a normal population. The distribution of temperature deviations about the mean approximate a normal distribution as illustrated in Figure 7. The variation of range with the number of observations is shown in Figure 8. The variation closely follows the expected value of the range drawn from a normal population.

7.2 Physical Dimensions of an Attractor

For a truly random, non-deterministic process, such as a variate drawn from a distribution unlimited on the left and right, the range will grow with

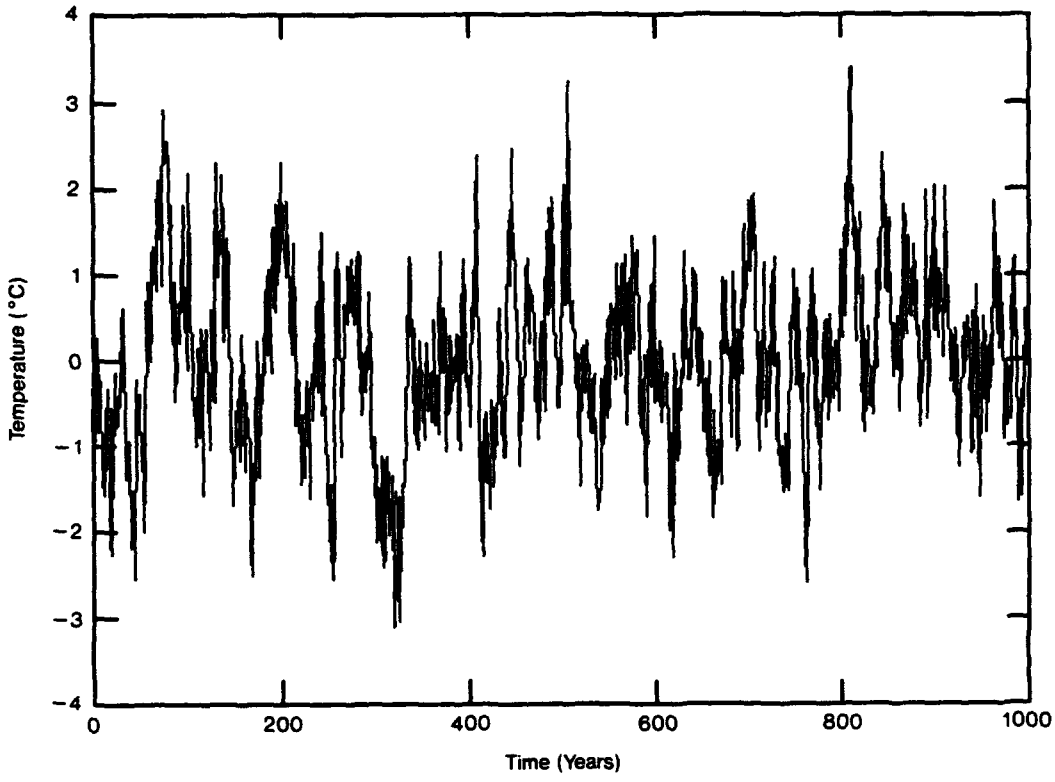

Figure 6. Variation of global-mean, annual-mean, sea-level air temperature for 1000 years in a numerical solution to the Lorenz 27-variable model of the atmosphere. Data are rated to unit variance and zero mean.

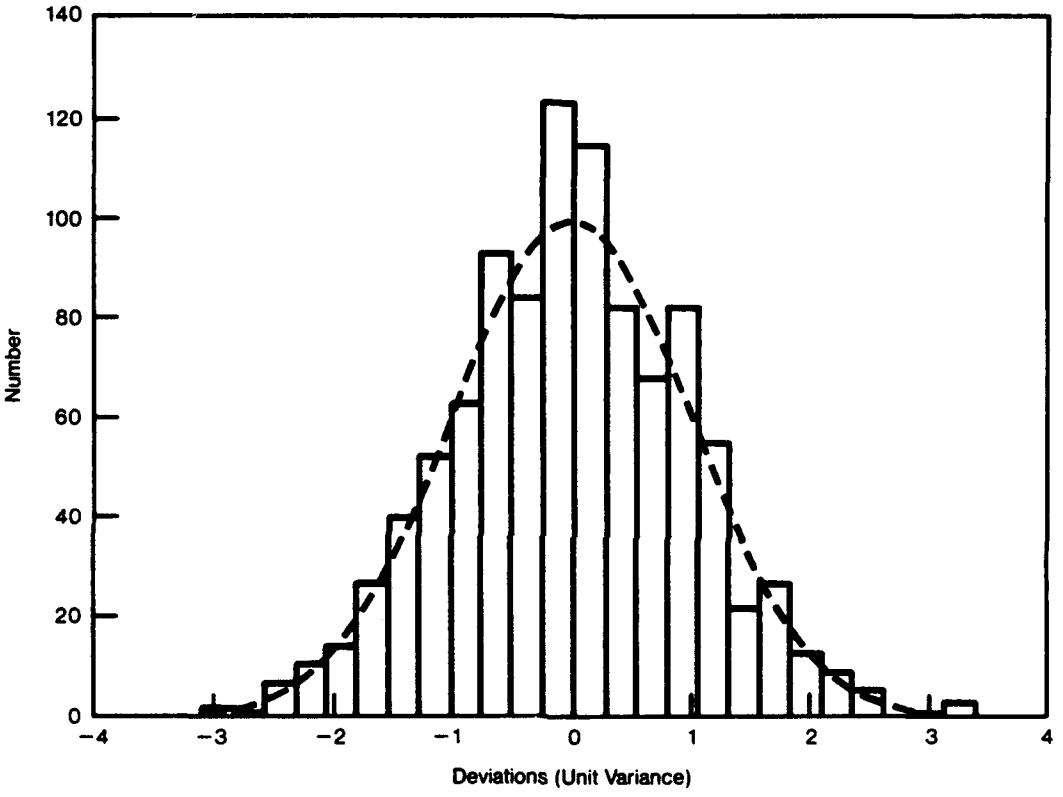

Figure 7. Distribution of global-mean, annual average temperatures for 1000 years of the Lorenz model.

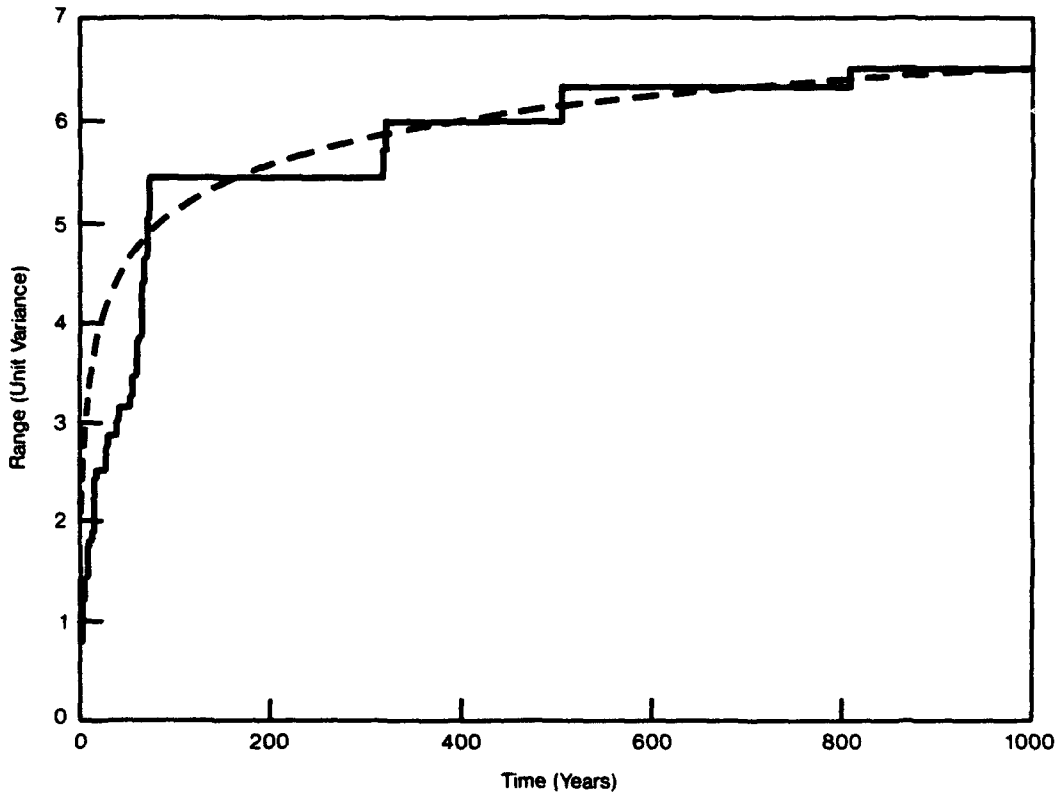

Figure 8. The variation with time of the range of global-mean, annual average temperature for the Lorenz model. The dotted curve gives the expected value for the range for samples drawn from a normal population.

the number of variates selected at a rate approximately

$$2(2\ ln\ n)^{1/2}.$$

For a time series n, the number of variates equals the number of time units. In a deterministic system governed by a set of coupled nonlinear differential equations, one would expect that the embodied conservation equations would set limits to the maximum growth of any state variable. In terms of the language of nonlinear dynamical systems, the governing attractor has finite physical dimensions. In this context we are speaking of the physical dimensions of the attractor as contrasted to the usual embedding dimensions which constitute a measure of the denseness of the set making up the attractor.

In the limit of large times, the range of random variables grows without bound but very slowly as $(ln\ n)^{1/2}$. For deterministic systems, the growth, as noted above, should be limited at a large enough n. For the Lorenz system, it is apparent that the limit has not been reached in 1000 years (see Figure 8). A general problem is that of determining the limits to the range of a particular variable and the time required to explore the far reaches of the attractor. It would appear that these are difficult issues, particularly for a system as complex as the 27-variable Lorenz system.

In order to further examine the time required for the Lorenz 27-variable model to explore the outer regions of the attractor, the model was run for 10,000 years. The results are shown in Figure 9. It would appear that the times to attain the outer reaches of the attractor are on the order of 5,000 years. To distinguish between a random process with the events drawn from a normal population and a deterministic Lorenz system by examining

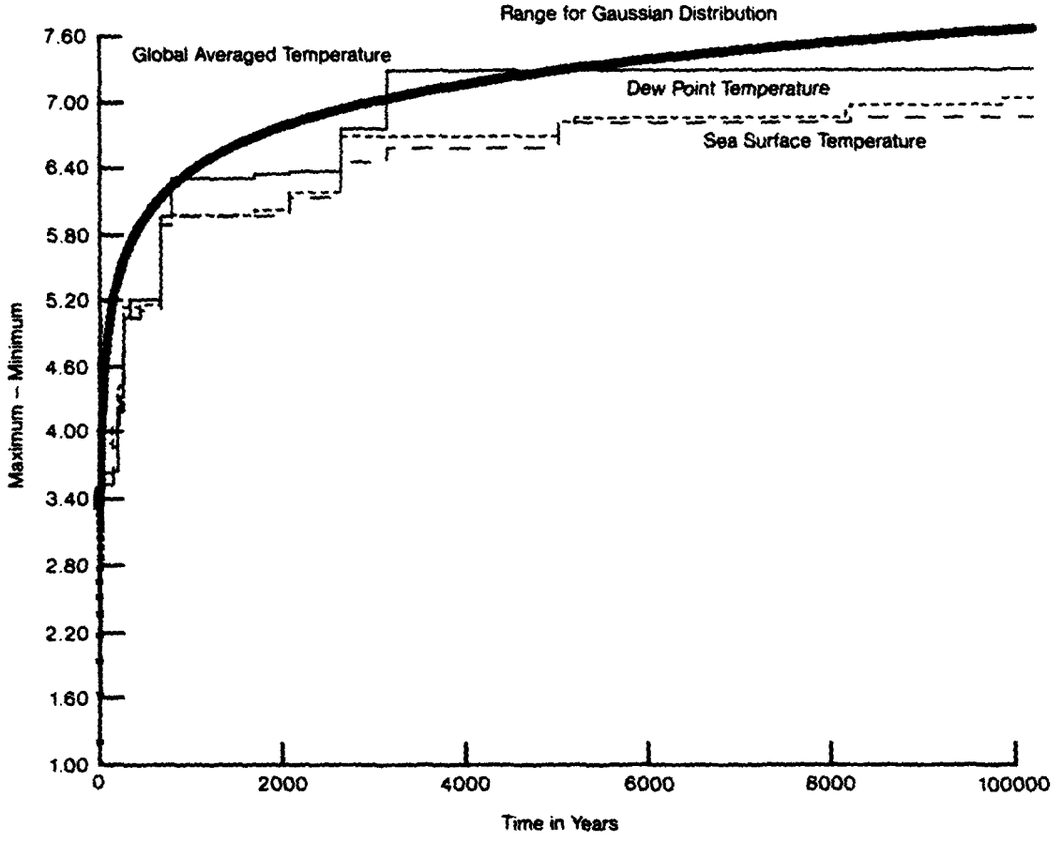

Figure 9. The variation with time of the range of the globally averaged values of surface atmosphere temperature, sea surface temperatures and dew point temperature. The values are averaged over a month and reported each year. The model is the Lorenz 27-variable model. The data are normalized to zero mean and unit variance. The heavy curve is the expected value of the range for a sample drawn from a normal population.

the tails of the distribution one would need to select on the order of 10^4 values. This observation suggests that before asymptotic behavior is reached by a dynamical system, transients of considerable duration can occur. Also shown in Figure 9 is the variation of the range of sea surface temperature and dew point temperature as calculated in the model. The tails of trails of the distribution of the parameters differ from that of a normal population, but very long times, on the order of 10^4 years, are required to reach the outer edges of the attractor. There is, of course, no guarantee that in any single integration the system will reach the boundary of the attractor. A further consideration is the random roundoff noise generated in the computer integration. This noise will cause the calculated range to mimic a random variable.

In a simple system, again one proposed by Lorenz (1984b), it does appear possible to obtain bounds on the maximum dimensions of the attractor. Lorenz (1984b) labels the following set of three coupled nonlinear equations as the simplest possible general circulation model:

$$\begin{aligned} \frac{dX}{dt} &= -Y^2 - Z^2 - aX + aF \\ \frac{dY}{dt} &= XY - bXZ - Y + G \\ \frac{dZ}{dt} &= bXY + XZ - Z. \end{aligned}$$

The variable X represents the strength of the large-scale westerly-wind current or the geostrophically equivalent equatorial-pole temperature gradient, while Y and Z are the strengths of the cosine and sine phases of a chain of superposed waves (Lorenz, 1984b). The quadratic terms containing b represent the translation of the waves by the western current. The remaining

quadratic terms represent a continual transfer of energy, except when X is negative, from the westerly flow to the waves.

The principal external driving force, the contrast between equatorial and pole heating, acts directly on the zonal flow X and is represented by a F. A secondary driving force, dependent on the difference between oceans and continents, enters the equations through G.

A section of the attractor for the Lorenz 84 model is displayed in Figure 10, which shows the range for the Z variable projected onto a plane including the Z axis and at an angle θ to the X axis. The motion is centered about $Z = 0$ but otherwise offset in X and Y.

We treat X, Y and Z, as coordinates in three-dimensional phase space. A rate of change of energy equation follows from the governing set by multiplying each by $2X, 2Y$, and $2Z$, respectively and summing

$$\frac{dR^2}{dt} = -[a(2X - F)^2 + (2Y - G)^2 + (2Z)^2 - (aF^2 + G^2)]/2$$

where $R^2 = X^2 + Y^2 + Z^2$ can be interpreted as the total energy - the sum of the kinetic, potential and internal energies. The right-hand side of the equation for $\frac{dR^2}{dt}$ vanishes on an ellipsoid

$$a(X - F/2)^2 + (Y - G/2)^2 + Z^2 = \frac{aF^2 + G^2}{4}.$$

The rate of change of energy outside the ellipsoid is negative. This implies that for any sphere centered on the origin in state space enclosing the ellipsoid, orbits passing through points outside the sphere will eventually pass through the sphere and remain inside. The ellipsoid is centered at (F/2, G/2,

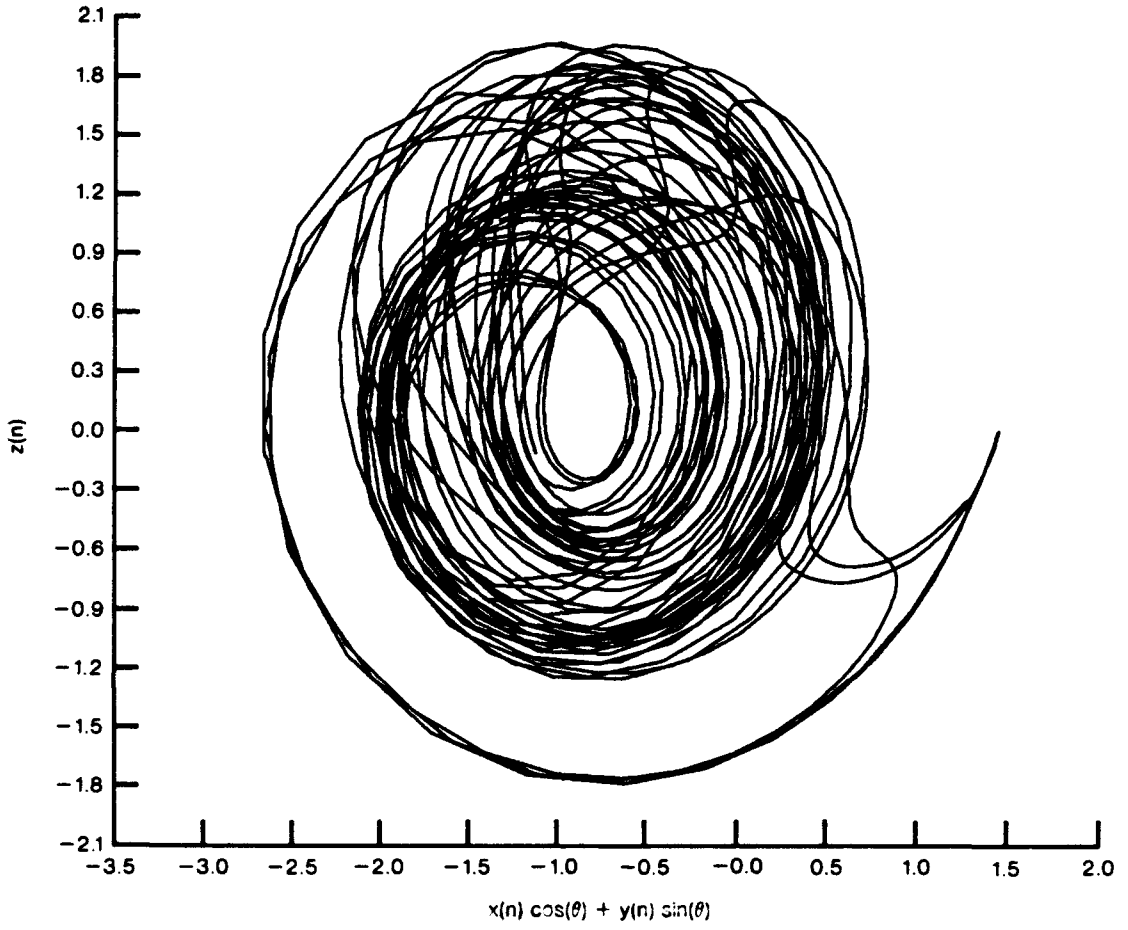

Figure 10. A section of the attractor for the Lorenz 3-variable model at a plane containing the z axis and at an angle of 117° to the x axis. The parameters for the model are given in Table 2.

Table 2

Maxima and Range for Variables Defined in Lorenz Lowest Order Central Circulation Model (F=8.0, G=1.0, a=0.25, b=4)

Variable	Maximum	Minimum
X	12.24	-0.12
Y	3.06	-1.06
Z	2.06	-2.06

0) with the corresponding major axes $((\frac{aF^2+G^2}{4a})^{1/2}, (\frac{aF^2+G^2}{4})^{1/2}, (\frac{aF^2+G^2}{4})^{1/2})$. The maxima and minima for the state variables are given in Table 2 for initial conditions lying within the ellipsoid and for specific values of the constants F, G and a. For initial conditions lying within the ellipsoid defined by $\frac{dR^2}{dt} = 0$, all orbits would be expected to remain within the ellipsoid, except for small inertial excursions, in the absence of noise. The ellipsoid provides the limits for values that can be taken on by the state variables. The constant b does not enter into the equation for the critical energy surface since b defines the strength by which the waves are carried by the zonal westerly current and does not alter the energy of the system.

The above analysis provides bounds on the maxima, minima and range attained by the state variables but provides no estimate of the average time required for a state variable to reach the boundary of the attractor. The only time scale within the systems of equations is determined by the constant a, the inverse of the decay time for the zonal current. Lorenz (1984b) assumes

a decay time for the zonal current of 20 days by selecting a=0.25 and taking 5 days as the unit time.

A numerical trial employing the constants shown in Table 2, taking the time unit to be 6 hours, averaging over 2.5 days and integrating from 34.25 years (5,000 points) yielded a variation in the X coordinate shown in Figure 11. The power spectrum and autocorrelation function for X, equivalent to the equator-pole temperature difference, are shown in Figures 12 and 13. The power spectrum displays much more structure than the Lorenz 27-variable model even though there is only one time scale that enters through the constant a. The distribution of values of X departs markedly from that a normal distribution (see Figure 14) in contrast to the Lorenz 27-variable model.

The maximum range observed in the data for X is 2.98, well within the limits shown in Table 2. In fact, in this particular run, the calculated orbits did not explore the outer edges of the attractor for the state variable X. The variation of the maximum range with time for X normalized to zero mean and unit variance is shown in Figure 15. Unlike the the Lorenz 27-variable model, the maximum range does not continue to climb with time but levels of well within the limits set by the critical energy surface.

The Y and Z state variables show similar behavior. The variation of Z with time is shown in Figure 16. The histogram (Figure 17) for the Z variable shows large deviation from a normal population. The range levels off with the maximum observed range of 4.17 (see Figure 18) slightly exceeding the maximum range expected for the Z variable of 4.12 (see Table 2). An

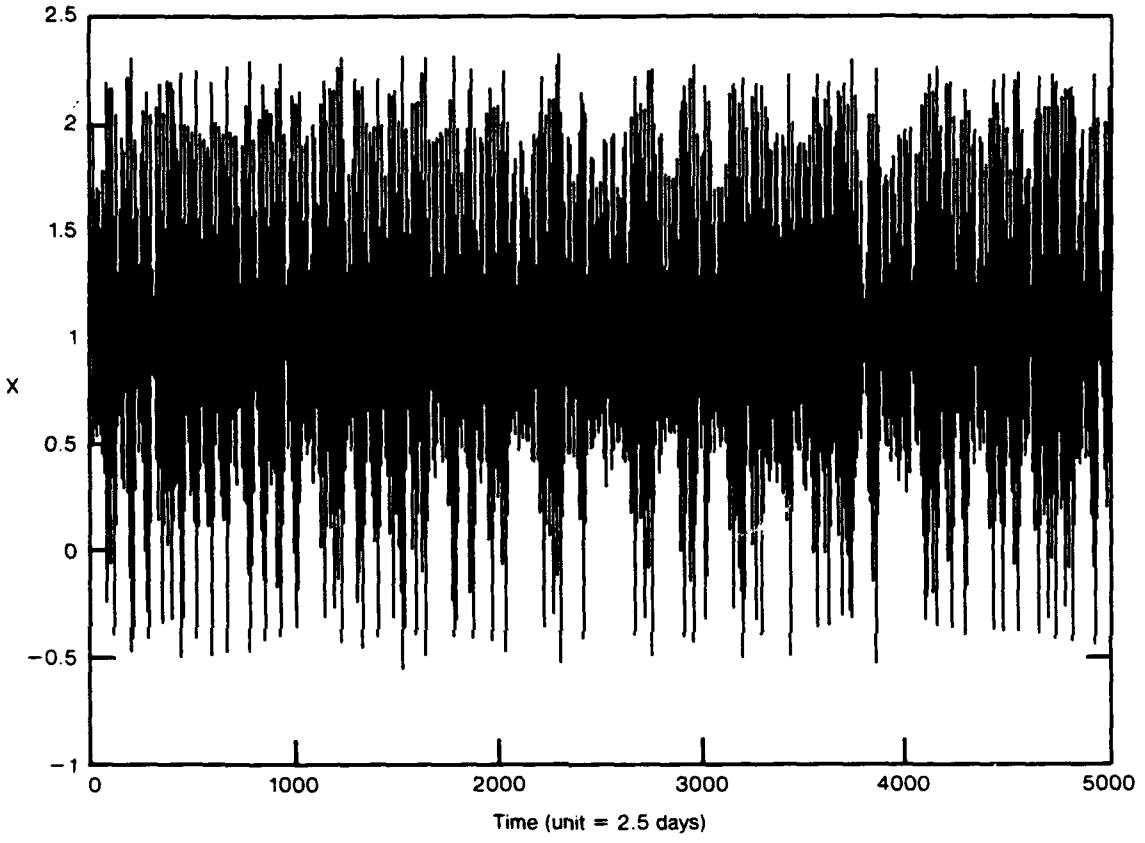

Figure 11. Variation of the Lorenz 3-variable model X coordinate (X is the equatorial-pole temperature gradient) with time for 12,500 days.

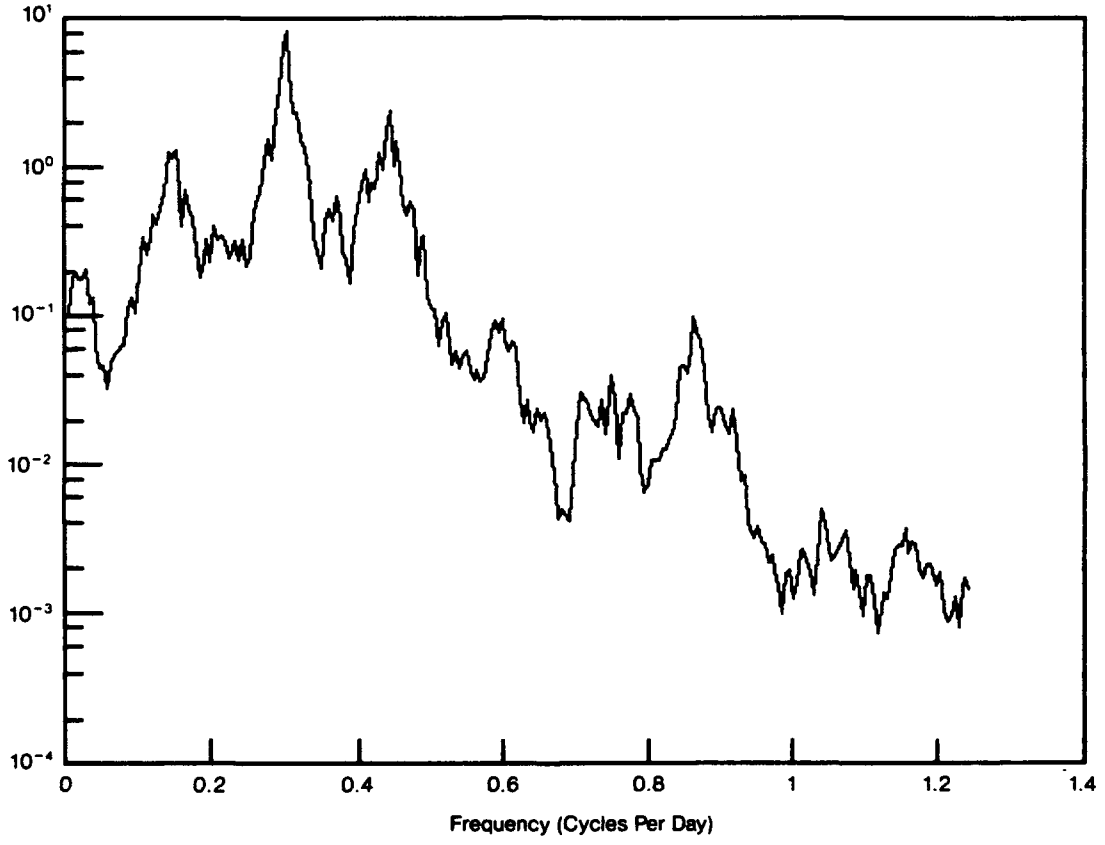

Figure 12. Power spectrum for state variable X in Lorenz 3-variable model. The data are normalized to zero mean and unit variance.

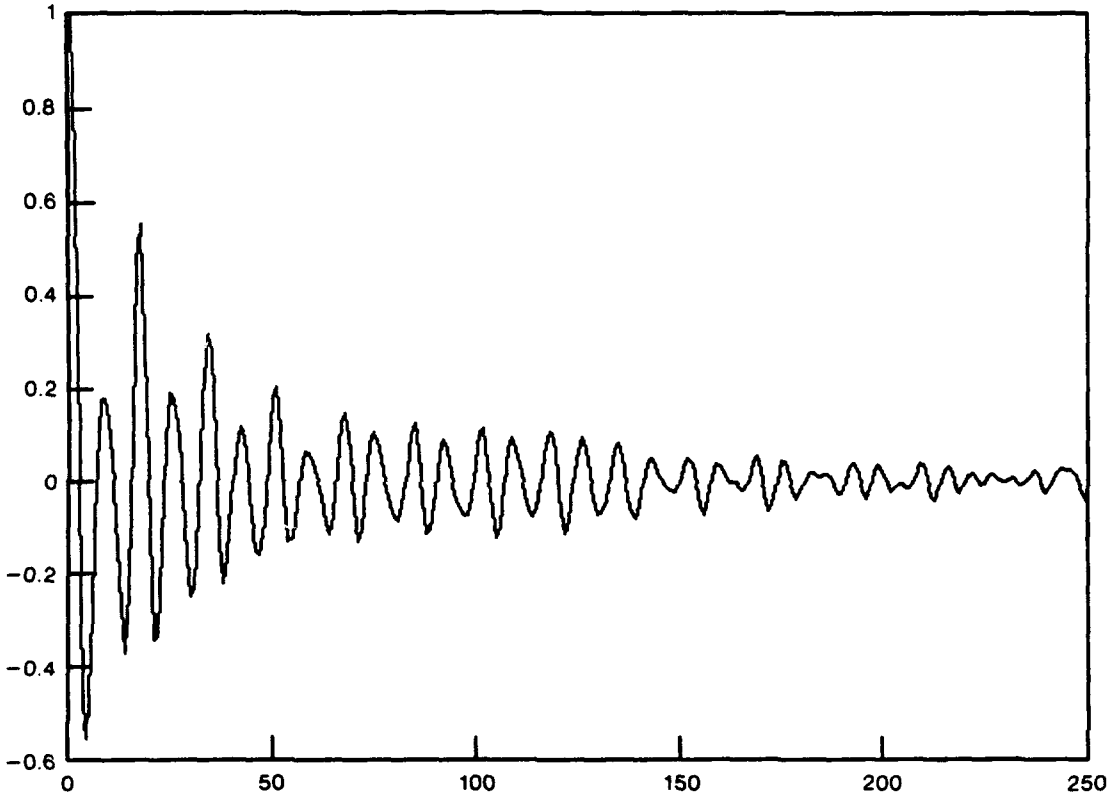

Figure 13. Autocorrelation junction for state variable X in Lorenz 3-variable model. The data are normalized to zero mean and unit variance.

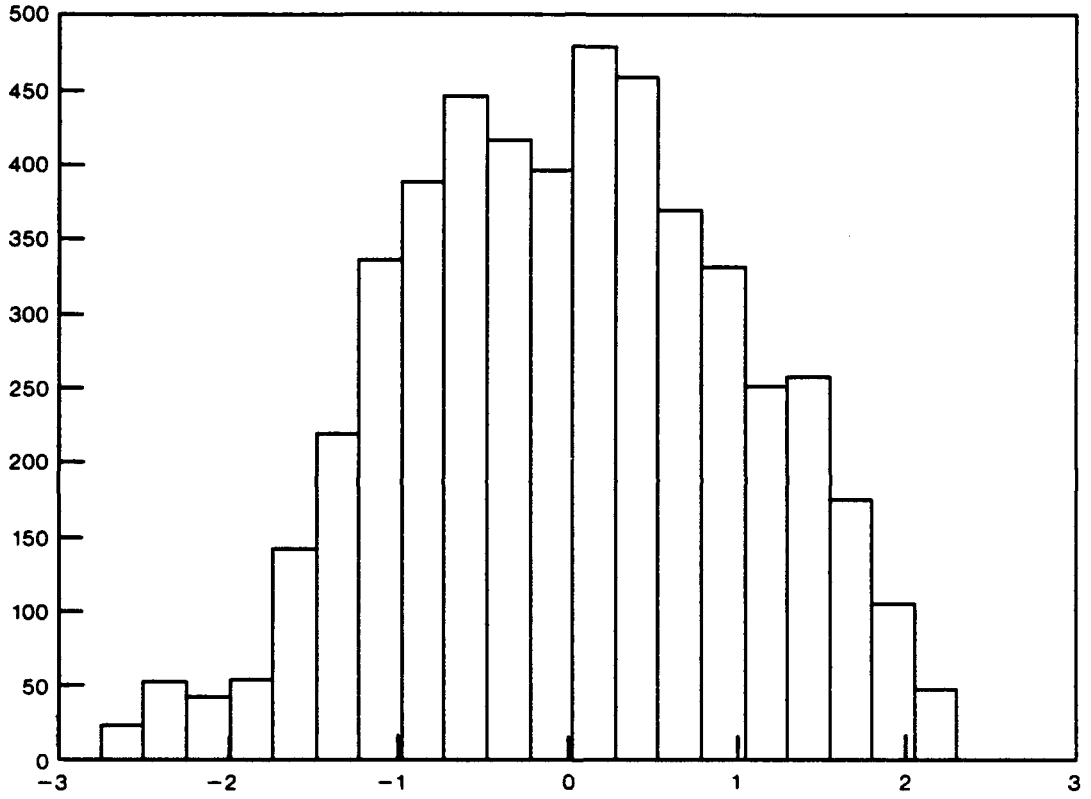

Figure 14. The distribution of value for the X state variable in the Lorenz 3-variable model. The data have been normalized to zero mean and unit variance.

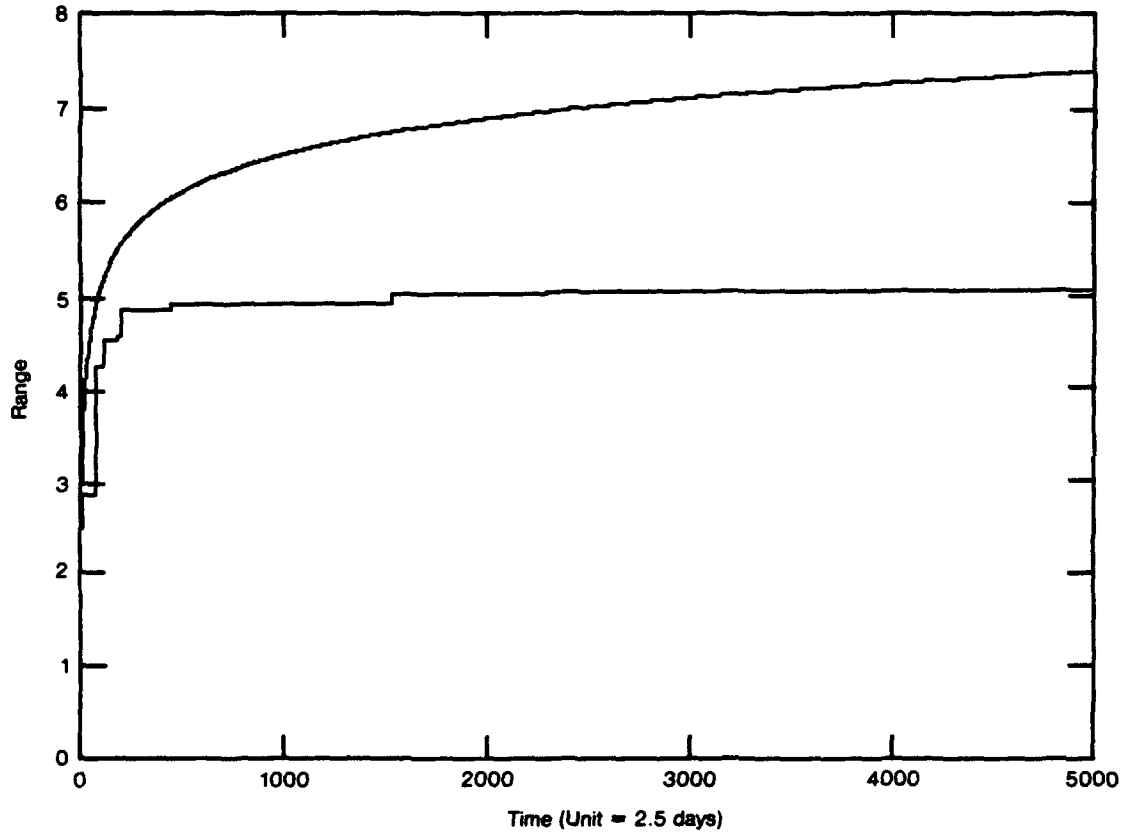

Figure 15. Variation of the range of the state variable X in the Lorenz 3-variable model. The data are normalized to zero mean and unit variance. The dotted line is the range expected for values chosen from a normal population with unit variance and zero mean.

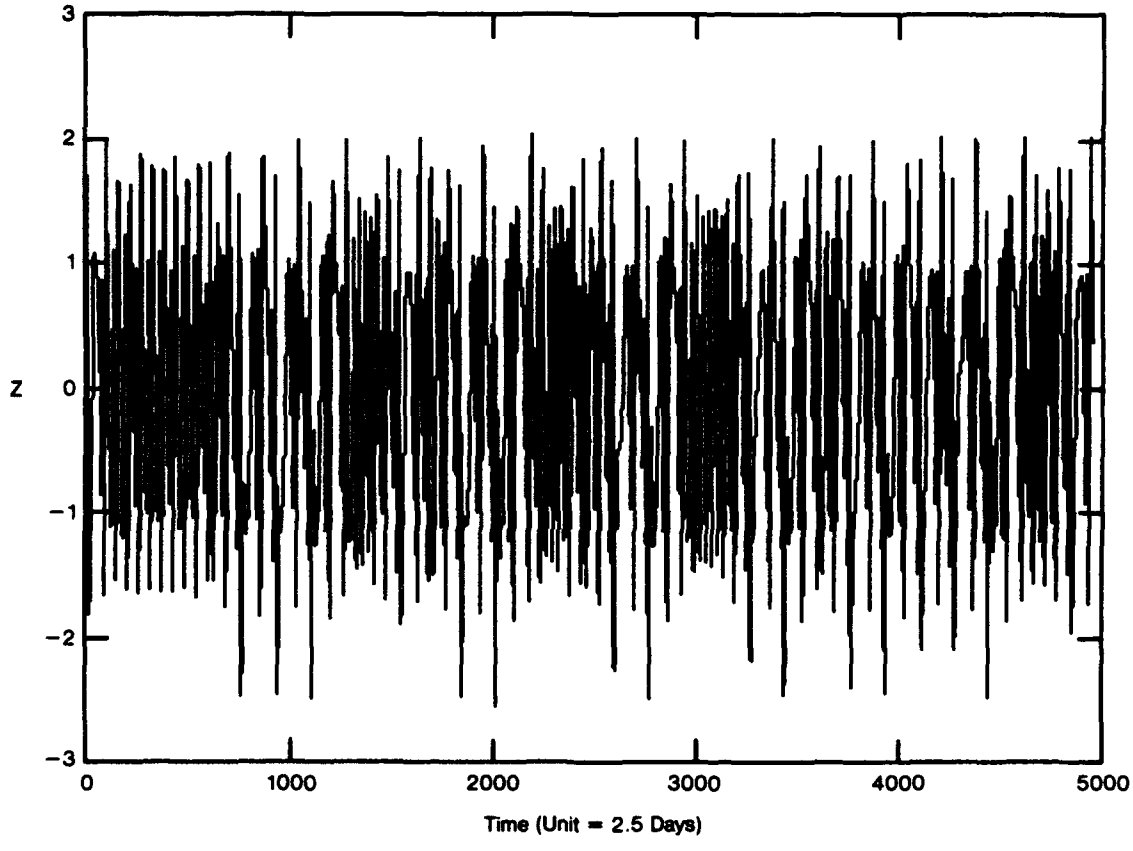

Figure 16. Variation of the Z state variable with time for the Lorenz 3-variable model. The unit of time is 2.5 days.

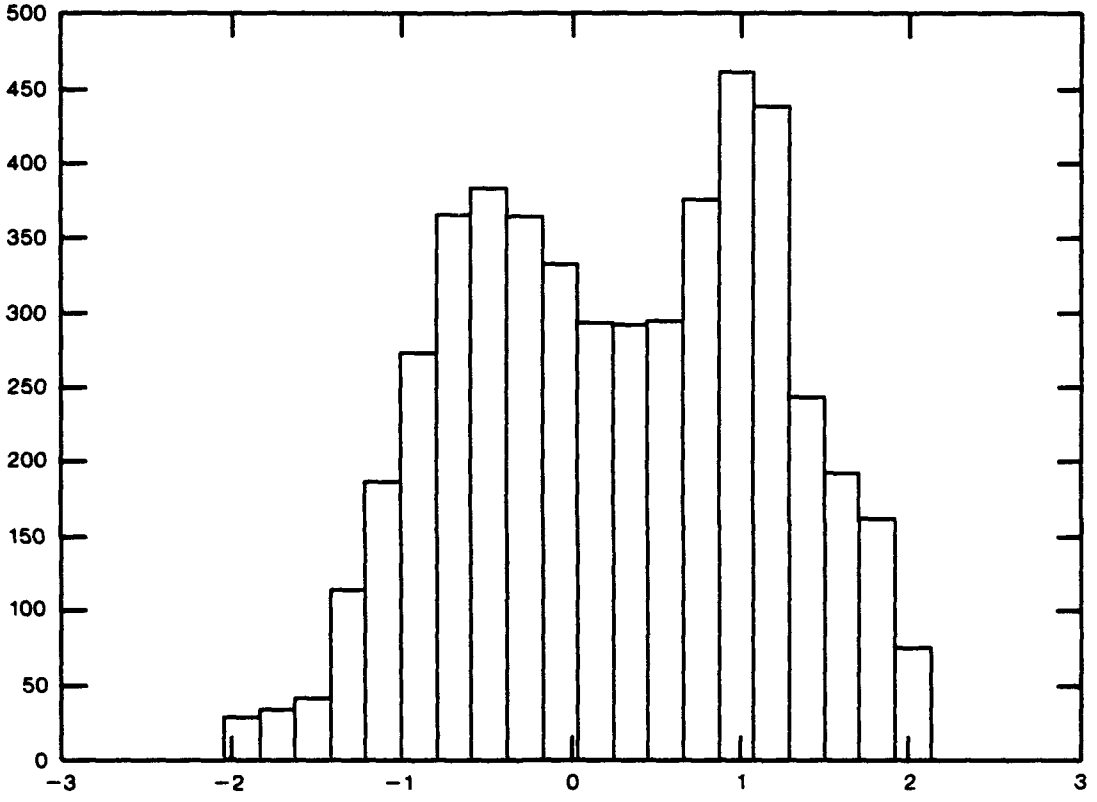

Figure 17. Histogram for the Z state variable in the Lorenz 1984 model.

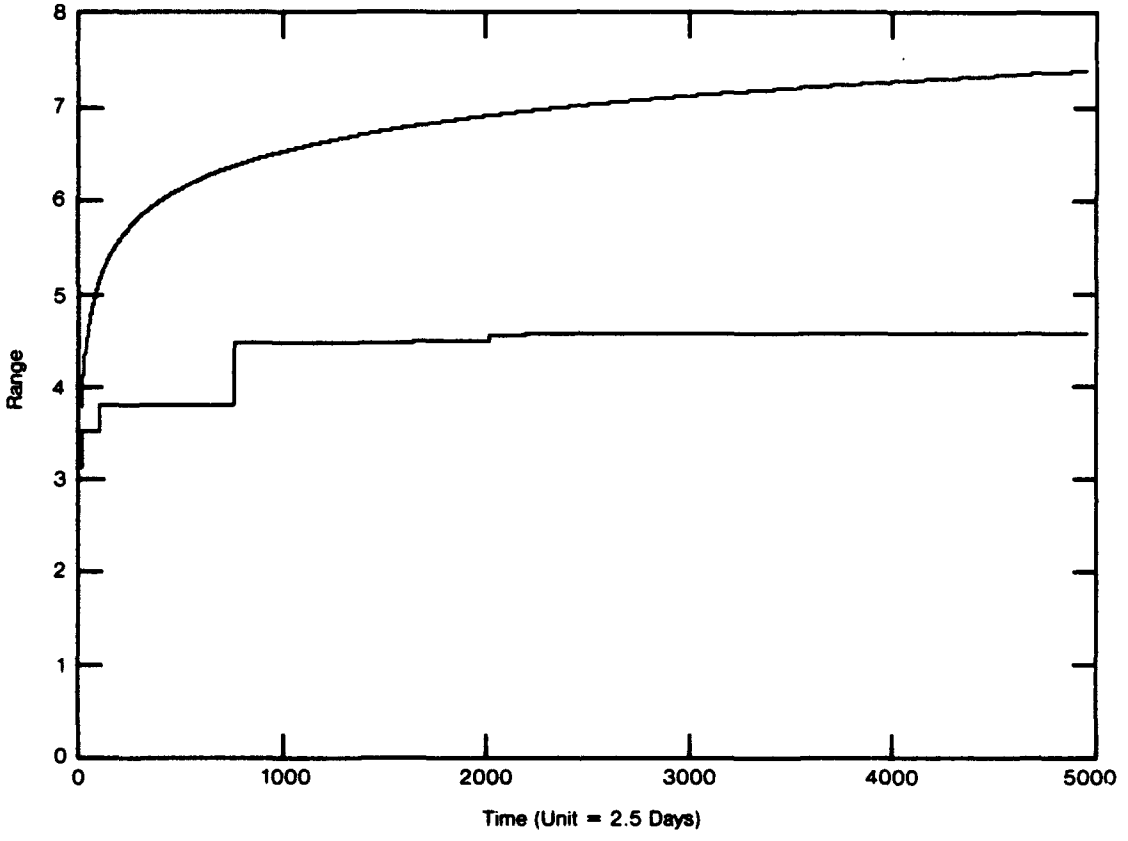

Figure 18. Range for the Z state variable in the Lorenz 1984 model. Data have been normalized to unit variance and zero mean. The curve represents expected range for a normally distributed variable.

observation of a value for the range slightly in excess of the maximum predicted range is not unexpected, since inertia will carry the the orbit outward before the inward pull of the attractor brings the orbit back within the limits of the critical energy surface.

The above example illustrates that it is possible to predict the maximum range of variables in a complex nonlinear system provided the equations are known. The limitation to the range of values which variables can assume likely comes from the conservation equations governing the motion. The time scale over which the maximum value may be attained is not determined by the above analysis.

7.3 Extremes for a Climate Model with a Linear Increase in Temperature

Levine etal., (1990) describe a version of the Lorenz 27-variable model in which the solar insolation is increased linearly with time leading to an increase of global temperature of 10° over a 1000-year period. The resulting temperature record is shown in Figure 19. The calculated variance is 9.24, which can be broken down into the part due to the linear increase and σ^2, the variance about the linearly increasing mean.

$$\begin{aligned} \text{Var} &\approx \frac{N^2 b^2}{12} + \sigma^2 \\ \sigma^2 &= 0.235 \end{aligned}$$

where N is the number of years and b is the rate of temperature increase.

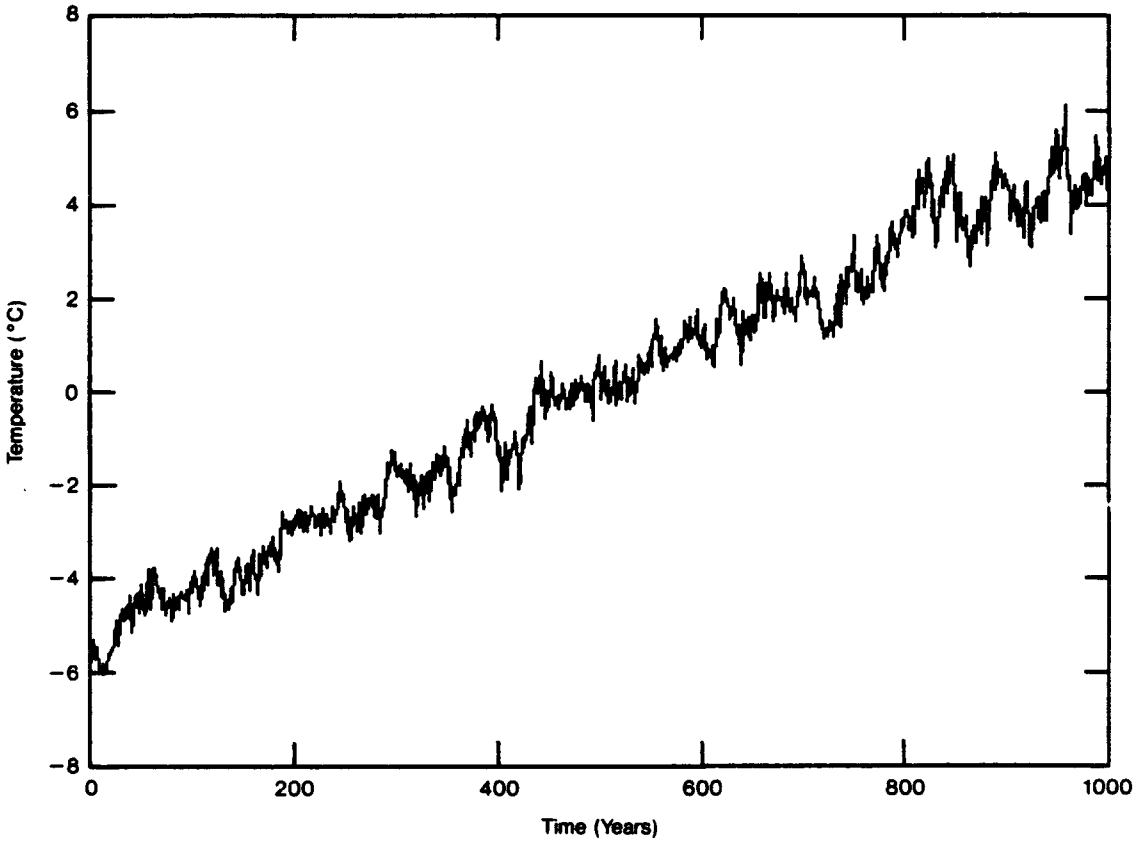

Figure 19. Global average temperature for Lorenz 27-variable model of the atmosphere in which the parameter corresponding to the insolation is increased linearly in time to provide an approximately 10°C increase in temperature over 1000 years.

The residual temperature curve after removing a trend by least squares is shown in Figure 20 with a distribution of the residuals approximating a normal distribution (see Figure 21). The maximum range after 1000 years for the residuals approximates the range expected by drawing variates from a normal population (see Figure 22). The removal of a trend before analyzing for extremes is a useful way of examining records of global average, surface air temperature records. There is a high probability that these records contain a linear trend (Levine et al. 1990).

7.4 Distribution of Extremes for Global Average Temperature Record

Our final example of an application of extreme value theory is to an annual average, global surface air temperature record. Three research groups (Jones, 1988; Hansen and Lebedeff, 1987, 1988; and Vinnikow et al., 1990) have produced similar analyses of hemispheric surface temperature variations from somewhat differing initial data sets. The longest of the data sets is that of Jones (1988) and we will use it in the analysis. An analysis of the Hansen-Lebedeff (1987, 1988) series (see Figure 1) produced results similar to those obtained from the Jones record. The Jones global average temperature variation is shown in Figure 23, which can be compared with Figure 1. Both figures show a relatively cool late 19th century followed by warming interrupted by cooling in the 1940-70 period (see Levine et al., 1990). The power spectrum for the Jones (1988) surface air temperature records is shown in Figure 24. The distribution of values for the Jones record is shown in Figure 25.

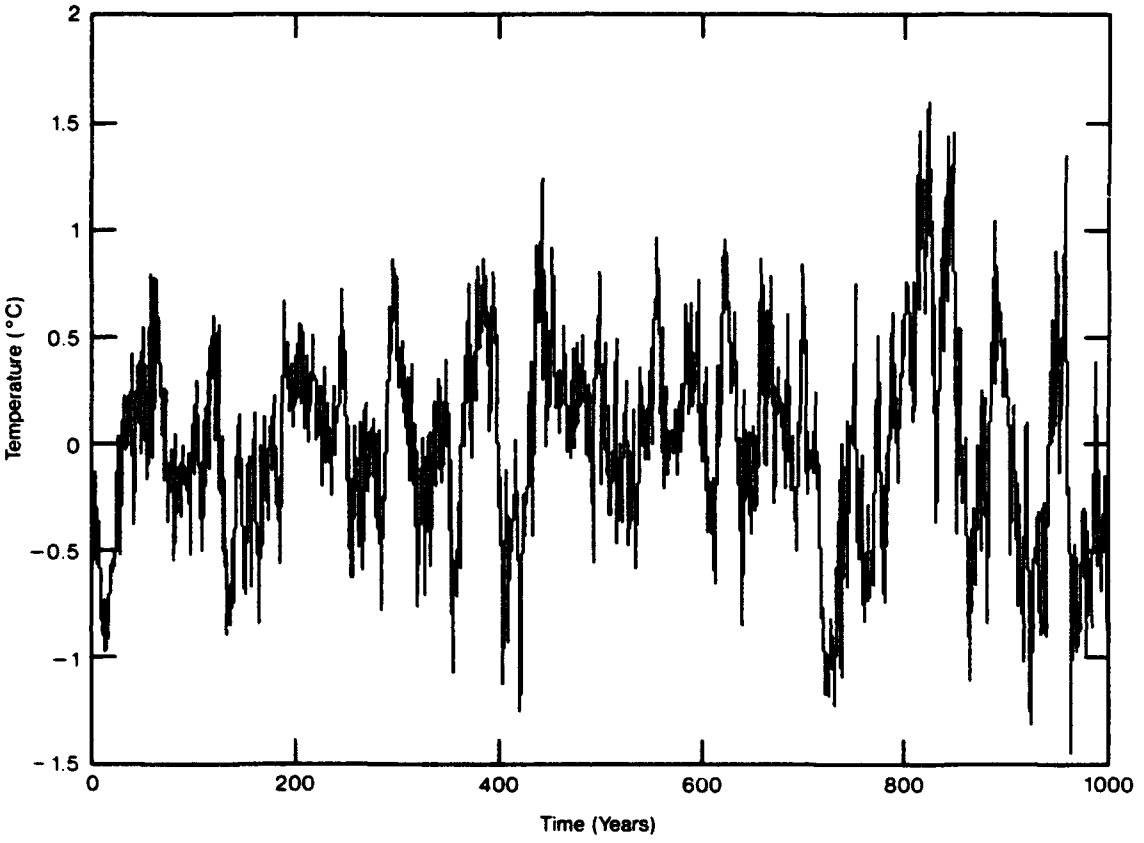

Figure 20. Residual temperatures after removing the trend by a least squares fit from Figure 17.

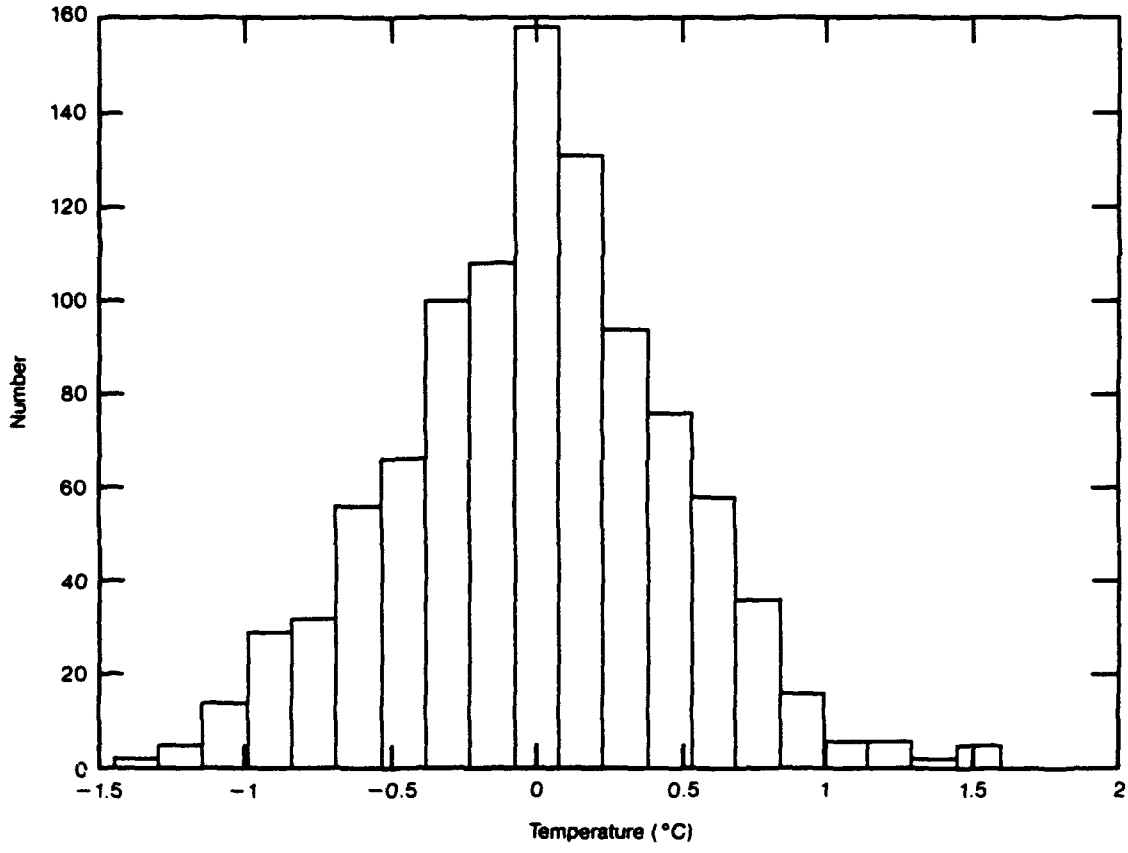

Figure 21. Distribution of values of the temperature for record shown in Figure 18.

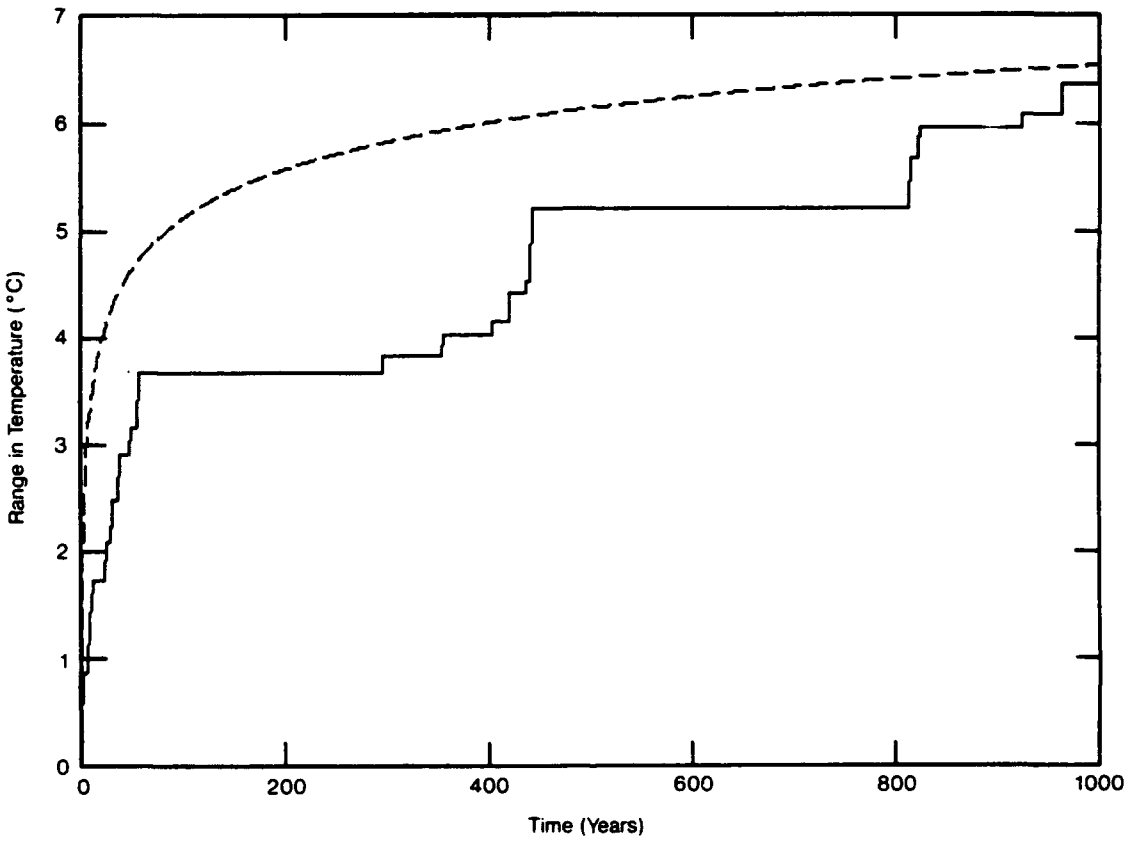

Figure 22. Range for the residuals for the Lorenz 27-variable system shown in Figure 20. The data have been normalized to zero mean and unit variance. The curve is the expected range for a normal population.

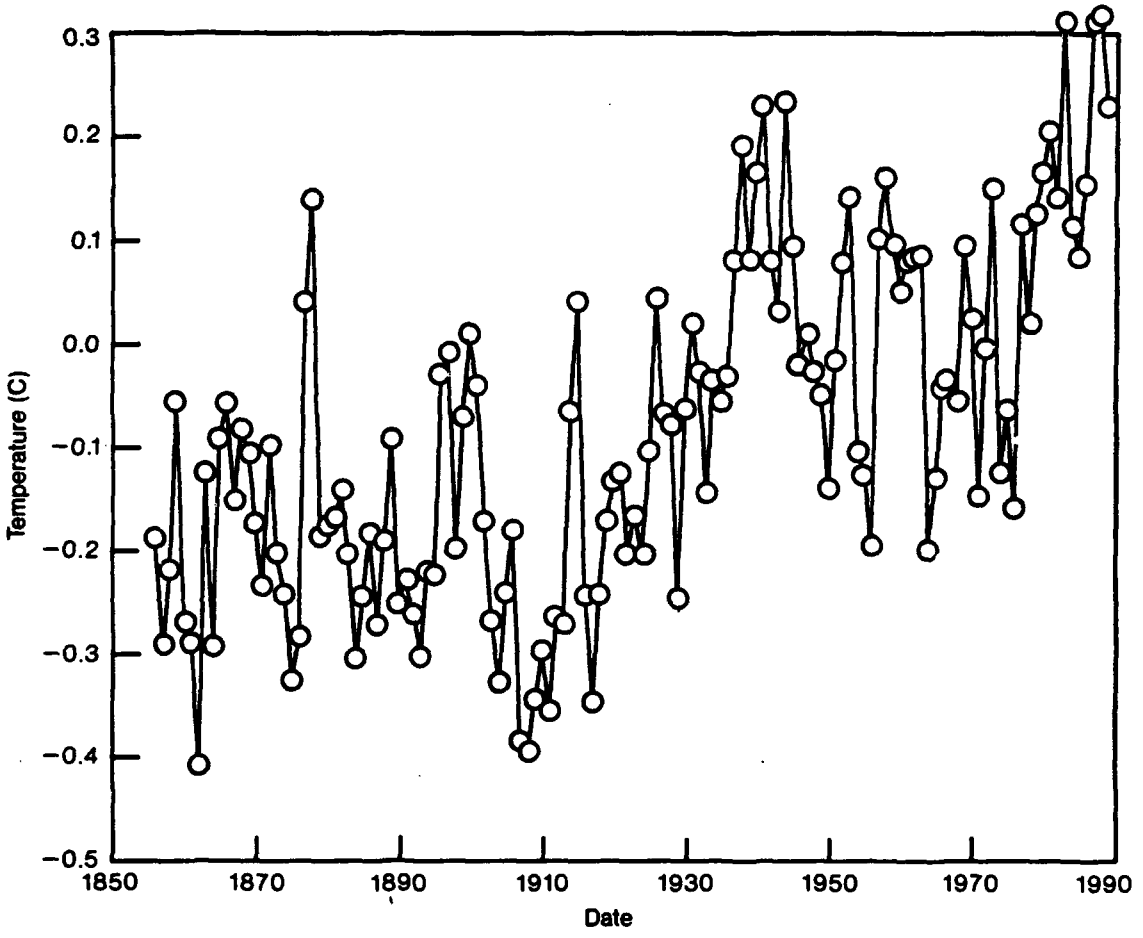

Figure 23. The variation of annual average global surface air temperature according to Jones (1988).

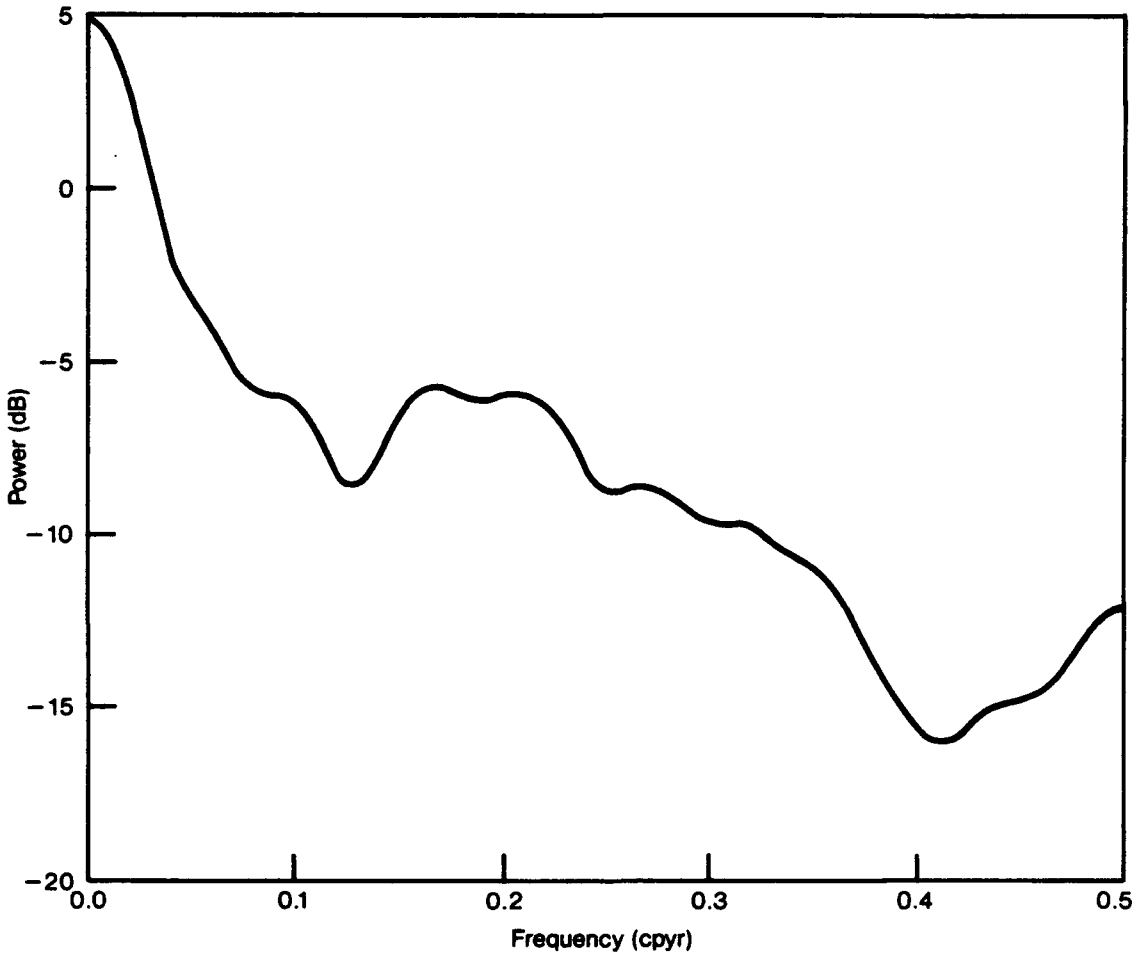

Figure 24. Power spectrum for the global annual average surface air temperature record shown in Figure 23. The data have been normalized to zero mean and unit variance.

The distribution differs from a normal distribution by being flatter. This is consistent with the observed trend of increasing temperature displayed in Figure 23 (a straight line would exhibit a uniform distribution of values). The range for the Jones record (see Figure 23) is shown in Figure 26. The deviations again are in the direction expected by a record containing a linear trend.

If a trend determined by least squares (slope = 0.28°C/century) is removed from the record, the resulting temperature residuals exhibit a histogram that closely approximates a normal distribution (see Figure 27). The tails of the distribution also approximate those of a normal variate, as is illustrated in Figure 28, which shows the variation of the range with time for the record exhibited in Figure 23 from which a linear trend has been removed.

The above analysis leads to the conclusion that once the linear trend is removed from the observed record, the distribution of the residuals both about the mean and in the tails approximates a normal distribution. In the Lorenz 27-variable system we observed chaotic behavior which led to a random (normally distributed) variation even over time scales of thousands of years. The observed data, even when temporally and spatially averaged, exhibit similar behavior. These observations suggest the possibility of chaotic noise at low frequency with important implications for predictability. In particular, records of less than 1000 years may show statistics indistinguishable from a random series (once trends assumed to be deterministic have been removed). Prediction, outside of the trend, may thus be impossible except in

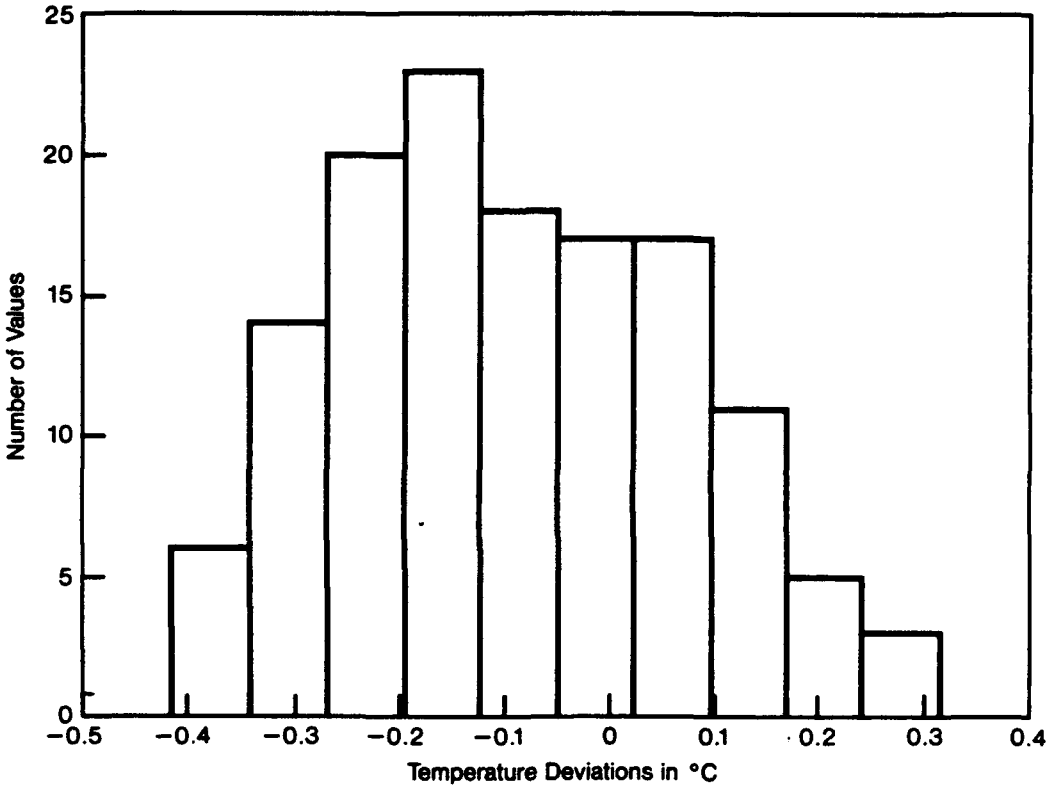

Figure 25. Histogram for global annual average surface air temperature record shown in Figure 23.

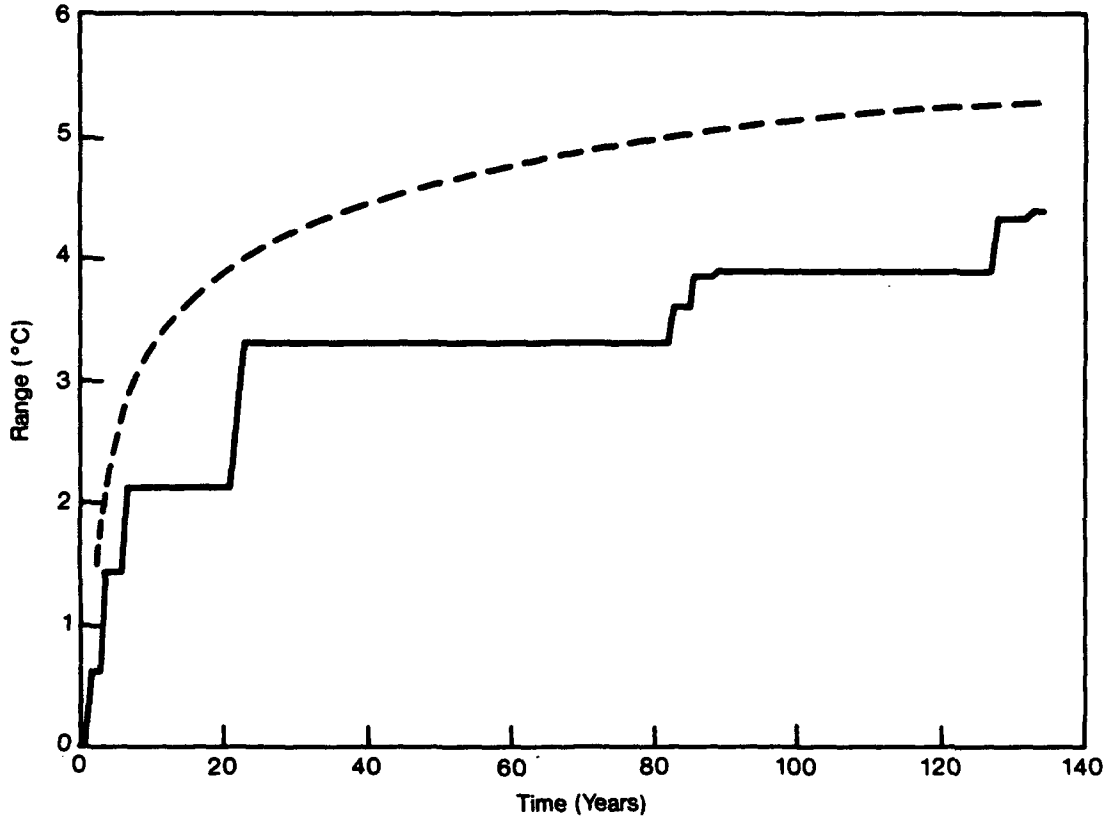

Figure 26. Variation of range for the global annual average surface air temperature record shown in Figure 23. The data have been normalized to zero mean and unit variance. The dotted line gives the expected value of the range for a normal variate.

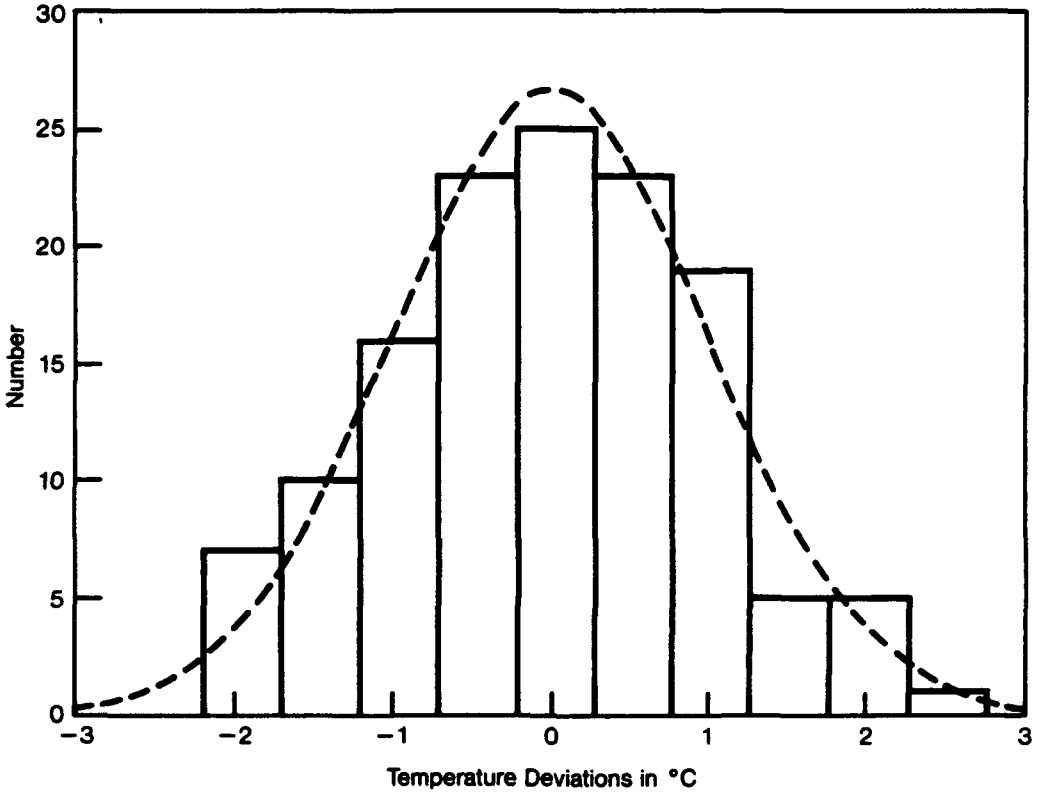

Figure 27. Histogram for the global annual average surface air temperature record after removal of a trend determined by a least squares fit. The residuals have been normalized to unit variance. The dotted line is the expected distribution of a normal variate.

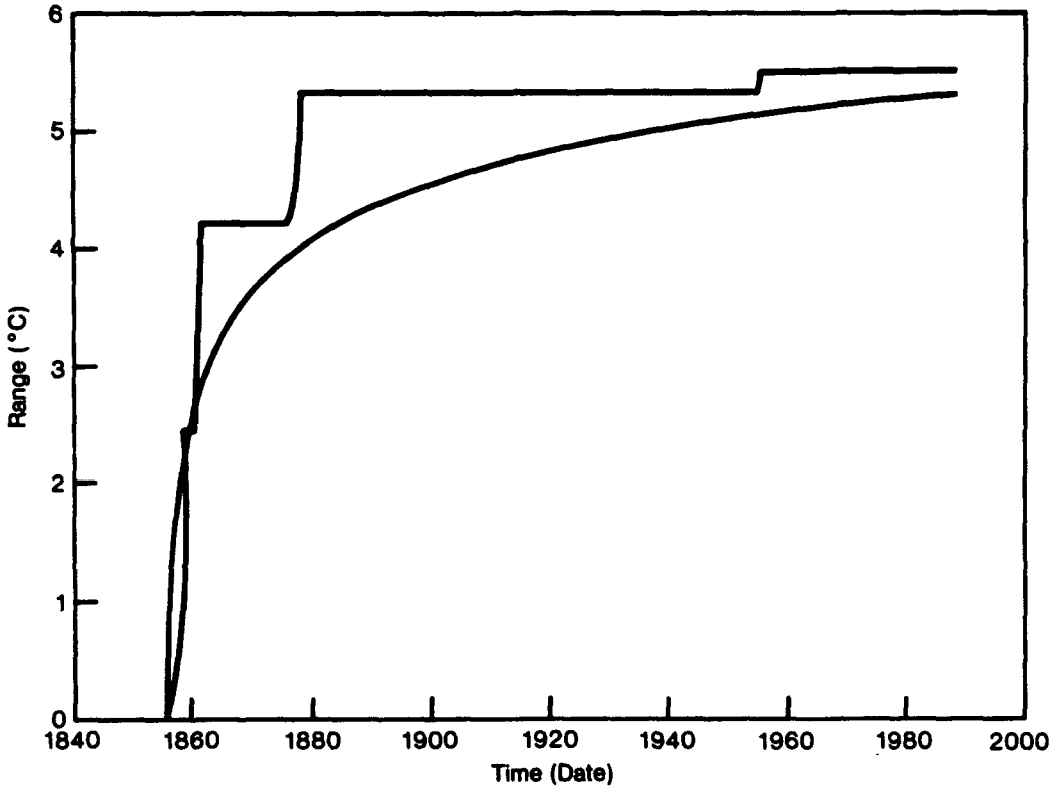

Figure 28. Variation of the range of the residual temperature obtained by removing the trend from the data displayed in Figure 23. The curve represents the expected range for a normally distributed variate.

a statistical sense. Similar considerations hold for models. The models may generate series that for time scales of a 1000 years have statistics identical to those of a random series. Using the models for deterministic prediction would in this case not be possible.

8 EFFECT OF A SHIFT OF THE MEAN ON THE FREQUENCY OF EXTREMES

The consensus view is that the greenhouse effect will bring about an overall warming of the planet, together with increased precipitation. But it is also anticipated that there will be strong regional variations with some regions cooling and others receiving less precipitation. The primary effect of these changes will be to shift the mean although there may also be changes in the variance other than those resulting from trends. The shift in mean can cause a large change in the probability of extreme events, as is evident from Figure 2. If over 100 years a particular climate parameter shifts by one-half a standard deviation toward lower or higher values, the initial probability of 0.5 becomes 0.05 or 0.95, respectively. The large-scale wind, temperature and moisture patterns in the atmosphere and the land and ocean changes associated with them undergo variations at all time scales from hours to billions of years. Some long-term changes have their origin in events that are external to the atmosphere-ocean system, such as variation in the earth's orbital parameters, volcanic explosions and changes in atmospheric composition. These long-term changes can accentuate or ameliorate the impact of shorter-term fluctuations which have their origin in chaotic noise. Alternatively, long-period chaotic noise might alter the local mean and carrys the short term fluctuations so that extreme values are reached. In this section we briefly consider the effect of shifts of the mean on the frequency of extremes.

The events of the Little Ice Age illustrate the impact of shifts in the

mean on extreme events. Parry and Carter (1985) have examined in detail the effect of short-term cool spells during the Little Ice Age on marginal agriculture in southwestern Scotland. In particular, they showed that small changes in the mean temperature associated with the Little Ice Age increased the frequency of damaging weather. Further, the probability of two successive bad years is even more sensitive to changes in the mean. The importance of successive extremes lies in their cumulative impact: an agricultural region may be able to understand a single shock, but if buffer stores are depleted by one bad season, a second one in succession may be far more devastating.

The longest available temperature record available to us is the one compiled by Manley (1974) for Central England from several discontinuous series. The record shows a number of isolated cool years (1740, 1782, 1860, 1979, 1922) and a clustering of two, three, or even more extremes in successive years (1673-75, 1688-98, 1838-40, 1887-88, 1891-92) as indicated in Figure 29. During the clustering of several cool summers in a row, when the temperature was marginal for the growth of oats, the farms at higher elevations in Scotland suffered greatly. One cool period, which persisted from 1688 to 1698, led to the abandonment of most of the farms above 300 m (Parry and Carter, 1985). Indeed, the "Seven Ice Years" of the 1690s caused catastrophe among rural populations in all of Northern Europe.

The effect of a change in the mean on the probability of an extreme event can be understood from a simple statistical model. The probability that some climate parameter (e.g., summer temperature, spring precipitation) falls above or below some threshold value for damage is P_1. In a stable climate

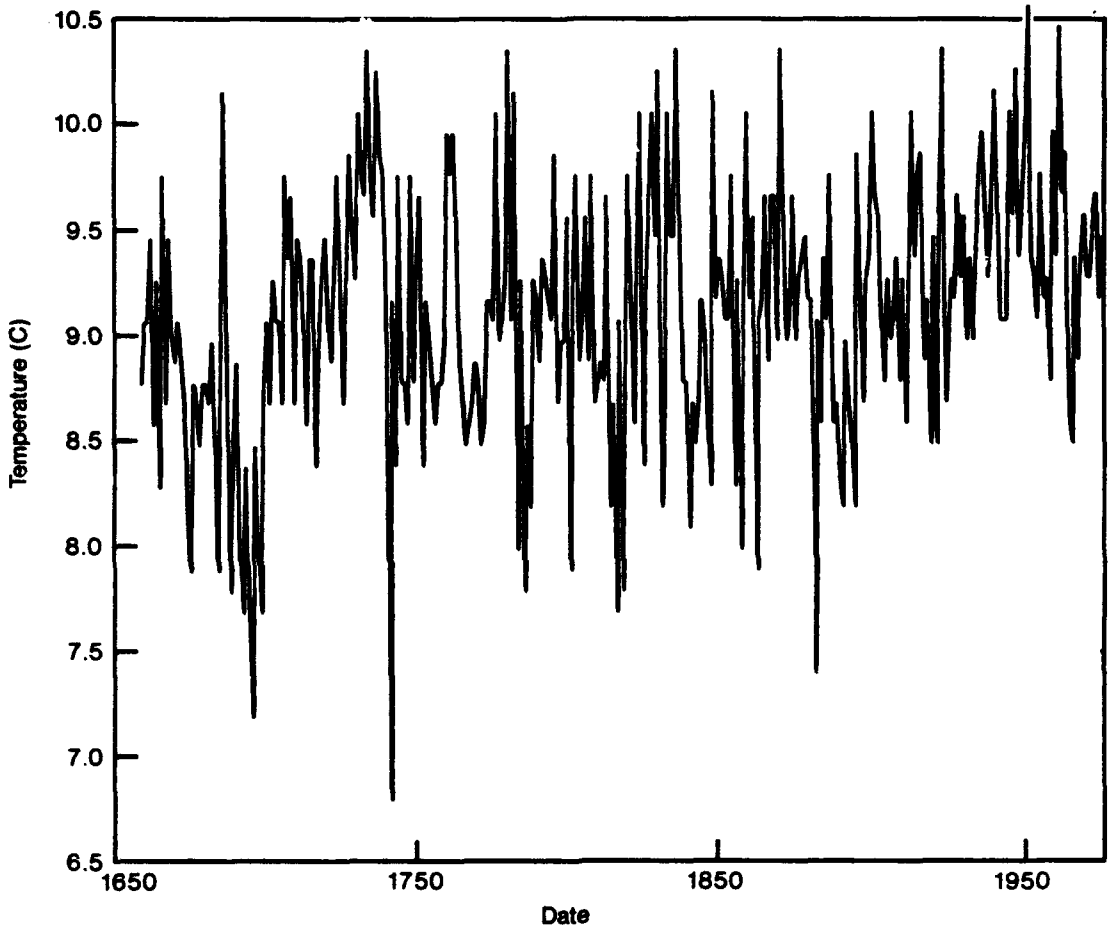

Figure 29. Variations in yearly average temperature in Central England. After Manley (1973).

regime the return period for the damaging event is P_I^{-1} years. Suppose that the climate shifts in such a way that the mean of the climate parameter shifts by X standard deviations toward the threshold value and that the climate parameter is normally distributed. The ratio of the probability in the shifted regime to that in the original regime, P_S/P_I, is a highly non-linear function of the shift of the mean, as is shown in Figures 30 and 31. If the initial probability is $P_I = 0.05$ (a return period of 20 years) and the mean is shifted by one standard deviation toward the threshold, then the subsequent probability is $P_S \simeq 0.25$, or a return period of four years. The probability of two successive years of an event with a return period of 20 years is only 1 in 400 in the initial state but moves to 1 in 16 in the shifted state. For example, the standard deviation for the temperature record of central England is 0.58°C, with a mean for the 1659-1977 period of 9.1°C. A decrease in the mean to 8.5°C would alter the probability of a once-in-100 years cool year to a once-in-12-years event. The long-period fluctuation in climate that comprised the Little Ice Age increased the probability of a short-term cool summer, making a sequence of successive cool summers much more likely than in the preceding or subsequent years.

Changes in the frequency of extreme high or low temperature, or of high or low precipitation, can be expected as climate shifts in response to greenhouse warming. The observed change in global average temperature of about 0.5° over the last century represents a shift of 2.3 standard deviations, making the probability of extremely warm global average years significantly higher.

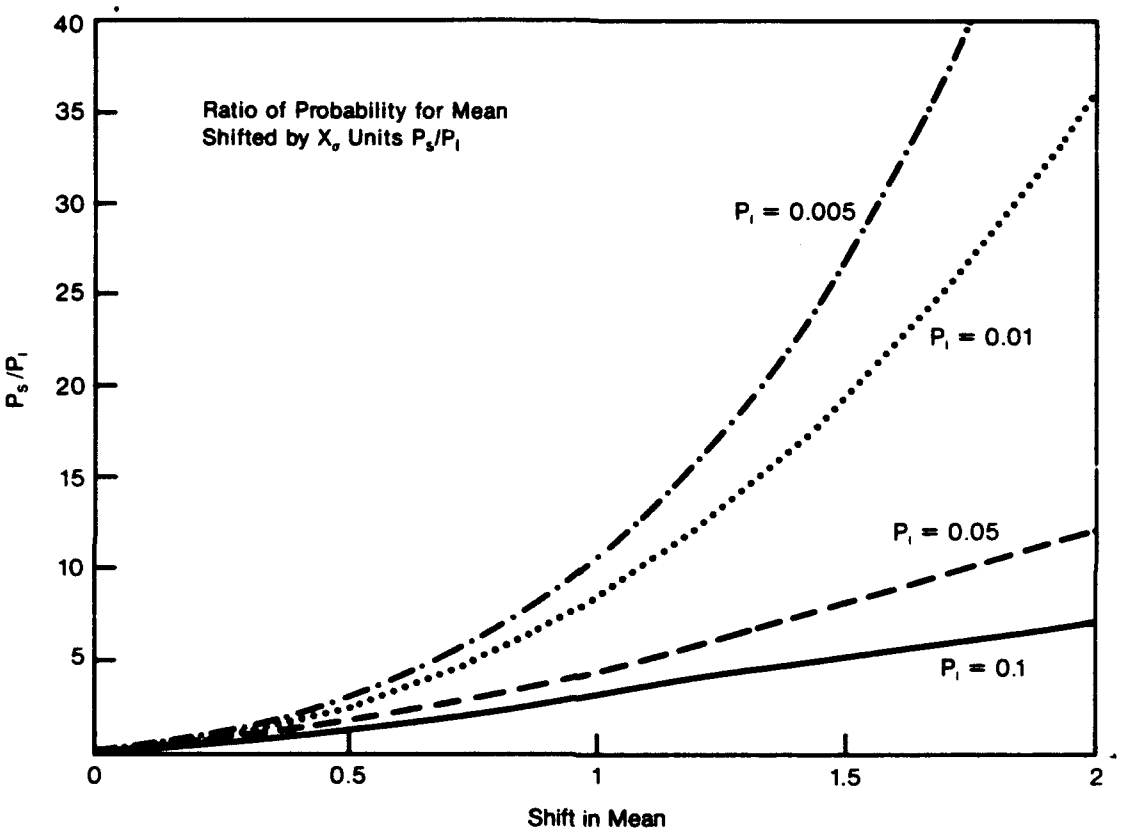

Figure 30. Ratio of probability of an extreme event to the probability of the event in the original, stable climate. Shift in mean measure is in terms of standard deviation. A normal population is assumed.

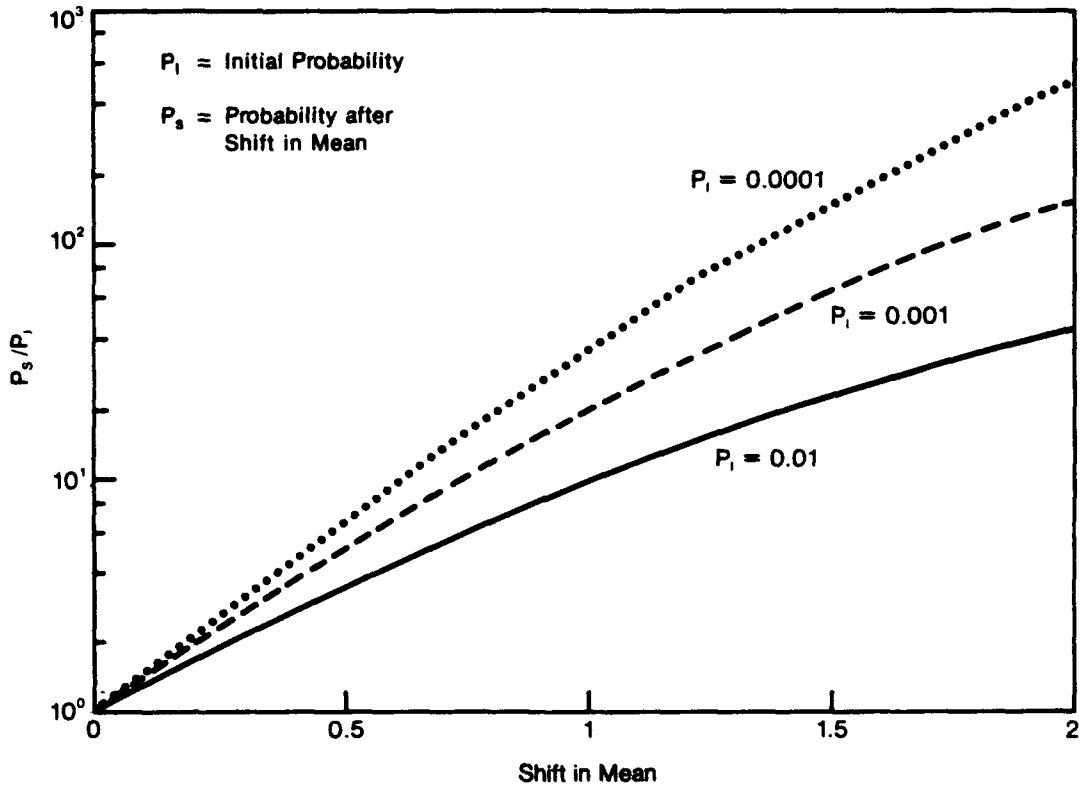

Figure 31. Shift in probability from a change in mean for initially rare events. Shift in mean is measured in terms of standard deviations, and a normal population is assumed.

9 SUMMARY

The statistical theory of extreme events can be applied in numerous ways to problems in climate change. Calculation of the range as a function of time can be used to detect the presence of a trend. The value of using extreme events in this application is that since they are rare, extreme events can be treated as independent without any assumption with respect to the underlying distribution. Analysis of the global annual average temperature record using extreme events and analysis based on an assumptions of an underlying normal distribution both confirm the existence of a trend with high odds ($10^5 - 10^6$) in favor of the trend hypothesis.

Analysis of observed long-term global annual average surface air temperature records and of model results show that both kinds of records are indistinguishable from a series of normally distributed variates once a trend is removed. For both kinds of records, the statistics approach those of normally distributed variates about the mean and in the tails of the distribution. For model results, this conclusion holds even for series that are several thousand years long. These observations cast doubt on the use of General Circulation Models to predict future climate deterministically .

The behavior of extreme values in nonlinear systems can be understood in terms of the physical dimensions of the underlying attractor. If the governing equations contain conservation laws, the outer boundary of the attractor lies within a manifold. The dimensions of the manifold define the limits to

the extreme values.

References

1. Cramér, H. (1946) Mathematical Methods of Statistics Princeton Univ. Press, Princeton, N.J.

2. Cramér, H. and M. Leadbetter (1967) Stationary and Related Processes, John Wiley, New York

3. David, H. (1981) Order Statistics, John Wiley, New York

4. Gumbel, E. J. (1958) Statistics of Extremes, Columbia Univ. Press, New York

5. Hansen, J. and S. Lebedeff (1987) Global trends of measured surface air temperature, J. Geophys. Res., **92**, 13345-13372

6. Hansen, J. and S. Lebedeff (1988) Global surface air temperature: Update through 1987, Geophys. Res. Letters, **15**, 323-326

7. Jones, P. (1988) Hemispheric surface air temperature variations: recent trends and an update to 1987, J. Clim. **1**, 654-660

8. Levine, H., G. MacDonald, O. Rothaus and F. Zachariasen (1990), Detecting Greenhouse Warming JASON Report JSR-89-330, MITRE Corp., McLean, Virginia

9. Leadbetter, M., C. Lindgren and H. Rootzen (1980) Extreme and Related Properties of Random Sequences and Processes, Springer-Verlag, New York

10. Lorenz, E. (1984a) Formulation of a low-order model of a moist general circulation model, J. Atmos. Sci. **41**, 1933-1945

11. Lorenz E. (1984b) Irregularity. A fundamental property of the elderly, Tellus, **30A**, 98-110

12. Manley, G. (1974) Central England temperatures: Monthly Means 1659-1973, Quart. J. Roy. Meteor. Soc., **100**, 389-405

13. Parry, M. and T. Carter (1985) The effects of climatic variations on agricultural risks, Climatic Change, **7**, 95-110

14. Vinnikov, K., Groisman and K. Lugina (1990) The empirial data on modern global climate change (temperature and precipitation), J. Clim., **3**, 622-677

DISTRIBUTION LIST

Dr Henry D I Abarbanel
Institute for Nonlinear Science
Mail Code R002/Building CMRR/Room 115
University of California/San Diego
La Jolla, CA 92093-0402

Director Ames Laboratory [2]
Iowa State University
Ames, IA 50011

Mr John M Bachkosky
Deputy DDR&E
The Pentagon
Room 3E114
Washington, DC 20301

Dr Joseph Ball
Central Intelligence Agency
Washington, DC 20505

Dr Arthur E Bisson
DASWD (OASN/RD&A)
The Pentagon
Room 5C675
Washington, DC 20350-1000

Dr Albert Brandenstein
Chief Scientist
Office of Natl Drug Control Policy
Executive Office of the President
Washington, DC 20500

Mr Edward Brown
Assistant Director
Nuclear Monitoring Research Office
DARPA
3701 North Fairfax Drive
Arlington, VA 22203

Dr Herbert L Buchanan III
Director
DARPA/DSO
3701 North Fairfax Drive
Arlington, VA 22203

Dr Curtis G Callan Jr
Physics Department
PO Box 708
Princeton University
Princeton, NJ 08544

Dr Ferdinand N Cirillo Jr
Central Intelligence Agency
Washington, DC 20505

Mr Phillip Colella
Dept of Mechanical Engineering
University of California/Berkeley
Berkeley, CA 94720

Brig Gen Stephen P Condon
Deputy Assistant Secretary
Management Policy &
Program Integration
The Pentagon Room 4E969
Washington, DC 20330-1000

DISTRIBUTION LIST

Ambassador Henry F Cooper
Director/SDIO-D
Room 1E1081
The Pentagon
Washington, DC 20301-7100

DARPA
RMO/Library
3701 North Fairfax Drive
Arlington, VA 22209-2308

Mr John Darrah
Senior Scientist and Technical Advisor
HQAF SPACOM/CN
Peterson AFB, CO 80914-5001

Dr Alvin M Despain
Electrical Engineering Systems
SAL-318
University of Southern California
Los Angeles, CA 90089-0781

Col Doc Dougherty
DARPA/DIRO
3701 North Fairfax Drive
Arlington, VA 22203

DTIC [2]
Defense Technical Information Center
Cameron Station
Alexandria, VA 22314

Mr John N Entzminger
Director
DARPA/TTO
3701 North Fairfax Drive
Arlington, VA 22203

CAPT Kirk Evans
Director Undersea Warfare
Space & Naval Warfare Sys Cmd
Code PD-80
Department of the Navy
Washington, DC 20363-5100

Mr F Don Freeburn
US Department of Energy
Code ER-33
Mail Stop G-236
Washington, DC 20585

Dr Dave Galas
Associate Director for
Health & Environmental Research
ER-70/GTN
US Department of Energy
Washington, DC 20585

Dr S William Gouse
Sr Vice President and General Manager
The MITRE Corporation
Mail Stop Z605
7525 Colshire Drive
McLean, VA 22102

LTGEN Robert D Hammond
CMDR & Program Executive Officer
US Army/CSSD-ZA
Strategic Defense Command
PO Box 15280
Arlington, VA 22215-0150

DISTRIBUTION LIST

Mr Thomas H Handel
Office of Naval Intelligence
The Pentagon
Room 5D660
Washington, DC 20350-2000

Maj Gen Donald G Hard
Director of Space and SDI Programs
Code SAF/AQS
The Pentagon
Washington, DC 20330-1000

Dr Robert G Henderson
Director
JASON Program Office
The MITRE Corporation
7525 Colshire Drive Z561
McLean, VA 22102

Dr Barry Horowitz
President and Chief Executive Officer
The MITRE Corporation
Burlington Road
Bedford, MA 01730

Dr William E Howard III [2]
Director For Space
and Strategic Technology
Office/Assistant Secretary of the Army
The Pentagon Room 3E474
Washington, DC 20310-0103

Dr Gerald J Iafrate
US Army Research Office
PO Box 12211
4300 South Miami Boulevard
Research Triangle Park, NC 27709-2211

Technical Information Center [2]
US Department of Energy
PO Box 62
Oak Ridge, TN 37830

JASON Library [5]
The MITRE Corporation
Mail Stop W002
7525 Colshire Drive
McLean, VA 22102

Dr George Jordy [25]
Director for Program Analysis
US Department of Energy
MS ER30 Germantown
OER
Washington, DC 20585

Dr O'Dean P Judd
Los Alamos National Lab
Mail Stop A-110
Los Alamos, NM 87545

Dr Steven E Koonin
Kellogg Radiation Laboratory
106-38
California Institute of Technology
Pasadena, CA 91125

Dr Chuck Leith
LLNL
L-16
PO Box 808
Livermore, CA 94550

DISTRIBUTION LIST

Dr Herbert Levine
Department of Physics
Mayer Hall/B019
University of California/San Diego
La Jolla, CA 92093

Technical Librarian [2]
Argonne National Laboratory
9700 South Cass Avenue
Chicago, IL 60439

Research Librarian [2]
Brookhaven National Laboratory
Upton, NY 11973

Technical Librarian [2]
Los Alamos National Laboratory
PO Box 1663
Los Alamos, NM 87545

Technical Librarian [2]
Pacific Northwest Laboratory
PO Box 999
Battelle Boulevard
Richland, WA 99352

Technical Librarian [2]
Sandia National Laboratories
PO Box 5800
Albuquerque, NM 87185

Technical Librarian [2]
Sandia National Laboratories
PO Box 969
Livermore, CA 94550

Technical Librarian [2]
Lawrence Berkeley Laboratory
One Cyclotron Road
Berkeley, CA 94720

Technical Librarian [2]
Lawrence Livermore Nat'l Lab
PO Box 808
Livermore, CA 94550

Technical Librarian [2]
Oak Ridge National Laboratory
Box X
Oak Ridge, TN 37831

Chief Library Branch [2]
AD-234.2 FORS
US Department of Energy
Washington, DC 20585

Dr Gordon J MacDonald
Institute on Global Conflict
& Cooperation
UCSD/0518
9500 Gilman Drive
La Jolla, CA 92093-0518

DISTRIBUTION LIST

Mr Robert Madden [2]
Department of Defense
National Security Agency
Attn R-9 (Mr Madden)
Ft George G Meade, MD 20755-6000

Dr Arthur F Manfredi Jr [10]
OSWR
Central Intelligence Agency
Washington, DC 20505

Mr Joe Martin
Director
OUSD(A)/TWP/NW&M
Room 3D1048
The Pentagon
Washington, DC 20301

Dr Nicholes Metropolis
Los Alamos National Laboratory
M/S B210
Los Alamos, NM 87545

Dr Julian C Nall
Institute for Defense Analyses
1801 North Beauregard Street
Alexandria, VA 22311

Dr William A Nierenberg
Director Emeritus
Scripps Institution of Oceanography
0221
University of California/San Diego
La Jolla, CA 92093

Dr Jerry North
College of Geosciences
Dept of Meteorology
Texas A&M University
College Station, TX 77843-3146

Dr Gordon C Oehler
Central Intelligence Agency
Washington, DC 20505

Oak Ridge Operations Office
Procurement and Contracts Division
US Department of Energy
(DOE IA No DE-AI05-90ER30174)
PO Box 2001
Oak Ridge, TN 37831-8757

Dr Peter G Pappas
Chief Scientist
US Army Strategic Defense Command
PO Box 15280
Arlington, VA 22215-0280

Dr Aristedes Patrinos [20]
Director of Atmospheric
& Climate Research
ER-74/GTN
US Department of Energy
Washington, DC 20585

Dr Bruce Pierce
USD(A)/D S
Room 3D136
The Pentagon
Washington, DC 20301-3090

DISTRIBUTION LIST

Mr John Rausch [2]
Division Head 06 Department
NAVOPINTCEN
4301 Suitland Road
Washington, DC 20390

Records Resources
The MITRE Corporation
Mailstop W115
7525 Colshire Drive
McLean, VA 22102

Dr Oscar S Rothaus
Math Department
Cornell University
Ithaca, NY 14853

Dr Fred E Saalfeld
Director
Office of Naval Research
800 North Quincy Street
Arlington, VA 22217-5000

Dr John Schuster
Technical Director of Submarine
and SSBN Security Program
Department of the Navy OP-02T
The Pentagon Room 4D534
Washington, DC 20350-2000

Dr Barbara Seiders
Chief of Research
Office of Chief Science Advisor
Arms Control & Disarmament Agency
320 21st Street NW
Washington, DC 20451

Dr Philip A Selwyn [2]
Director
Office of Naval Technology
Room 907
800 North Quincy Street
Arlington, VA 22217-5000

Dr Albert Semtner
Department of Oceanography
Naval Post Grad School
Code 68
Monterey, CA 93949

Superintendent
CODE 1424
Attn Documents Librarian
Naval Postgraduate School
Monterey, CA 93943

Dr George W Ullrich [3]
Deputy Director
Defense Nuclear Agency
6801 Telegraph Road
Alexandria, VA 22310

Ms Michelle Van Cleave
Asst Dir/National Security Affairs
Office/Science and Technology Policy
New Executive Office Building
17th and Pennsylvania Avenue
Washington, DC 20506

Dr John Fenwick Vesecky
Dir Space Physics Res Lab
University of Michigan
1424A Space Research Bldg
Ann Arbor, MI 48109-2143

DISTRIBUTION LIST

Mr Richard Vitali
Director of Corporate Laboratory
US Army Laboratory Command
2800 Powder Mill Road
Adelphi, MD 20783-1145

Dr Edward C Whitman
Dep Assistant Secretary of the Navy
C3I Electronic Warfare & Space
Department of the Navy
The Pentagon 4D745
Washington, DC 20350-5000

Mr Donald J. Yockey
U/Secretary of Defense
For Acquisition
The Pentagon Room 3E933
Washington, DC 20301-3000

Dr Linda Zall
Central Intelligence Agency
Washington, DC 20505

Mr Charles A Zraket
Trustee
The MITRE Corporation
Mail Stop A130
Burlington Road
Bedford, MA 01730